



# Design, synthesis, and SAR study of highly potent, selective, irreversible covalent JAK3 inhibitors

Linhong He<sup>1,2</sup> · Mingfeng Shao<sup>1</sup> · Taijin Wang<sup>1</sup> · Tingxuan Lan<sup>1</sup> · Chufeng Zhang<sup>1</sup> · Lijuan Chen<sup>1</sup>

Received: 29 April 2017 / Accepted: 13 December 2017  
© Springer International Publishing AG, part of Springer Nature 2018

## Abstract

Here, we report the design and synthesis of pyrimidinyl heterocyclic compounds containing terminal electrophiles as irreversible covalent JAK3 inhibitors that exploit a unique cysteine (Cys909) residue in JAK3. Investigation of the structure–activity relationship utilizing kinase assays resulted in the identification of potent and selective JAK3 inhibitors such as **T1**, **T8**, **T15**, **T22**, and **T29**. Among them, **T29** was verified as a promising JAK3 irreversible inhibitor that possessed the best bioactivity and selectivity against JAKs and kinases containing a cysteine in the residue analogous to Cys909 in JAK3, suggesting that covalent modification of this Cys residue allowed the identification of a highly selective JAK3 inhibitor. Moreover, **T29** also displayed a significant anti-inflammatory effect in ICR mice through the inhibition of increased paw thickness, which is worth further optimization to increase its potency and medicinal properties.

**Keywords** JAK3 · Covalent inhibitor · Selectivity · Structure–activity relationship (SAR) · Docking

## Abbreviations

JAK	Janus kinase
STAT	Signal transducer and activator of transcription
Cys	Cysteine
SAR	Structure–activity relationship

## Introduction

The Janus kinases (JAKs) are a family of four cytoplasmic nonreceptor tyrosine kinases (JAK1, JAK2, JAK3, and TYK2) that play important roles in the signaling of various cytokines [1–3]. Upon activation through cytokine signaling, JAKs subsequently activate the downstream sig-

nal transducer and activator of transcription (STAT) family of transcription factors, which ultimately regulate target gene expression that governs cell proliferation and survival [4,5]. The JAK/STAT signaling pathway is involved in a variety of biological processes, including the regulation of immune and inflammatory responses [5–7].

Biochemical and genetic studies have identified that JAK3 is restrictedly expressed in lymphoid tissue and is only activated by cytokines of  $\gamma_c$  subfamily (IL-2, IL-4, IL-7, IL-9, IL-15, and IL-21), while the other JAK family members widely express and are activated by numerous cytokines [8–10]. Although JAK3 deficiency in humans or mice can result in severe combined immunodeficiency (SCID) due to the complete abrogation of IL-2, IL-4, IL-7, IL-9, IL-15, and IL-21 signaling in T cells and NK cells, these cases are only limited to immune cells [5,11]. Moreover, heterozygous parents of SCID patients do not exhibit immune-compromised phenotypes, suggesting that partial inhibition of JAK3 can be used to modulate immune responses [6,8]. This also has been applied in several important clinical practices, such as the prevention of transplant rejection and the treatment of various autoimmune disorders [6,8]. Taking these findings together, selective targeting of JAK3 has long been viewed as a potent strategy for the treatment of immune system indications while avoiding unexpected side effects caused by inhibition of other JAKs [8,12,13].

**Electronic supplementary material** The online version of this article (<https://doi.org/10.1007/s11030-017-9803-2>) contains supplementary material, which is available to authorized users.

✉ Lijuan Chen  
clijuan125@163.com

<sup>1</sup> Cancer Center, West China Hospital, Sichuan University and Collaborative Innovation Center, # 17, Section 3, Ren Min Nan Lu, Chengdu 610041, People's Republic of China

<sup>2</sup> Department of Pharmacology, School of Pharmacy, Guangxi Medical University, # 22 Shuangyong Road, Nanning 530021, Guangxi, People's Republic of China

**Table 1** Sequence conservation of human Janus kinase active sites

Position (in JAK3)	904	905	906	907	908	<b>909</b>	912	940	945	947	948	953	954	956	965	966
JAK3	Y	L	P	S	G	<b>C</b>	D	L	C	H	R	R	N	L	I	A
JAK1	F	L	P	S	G	<b>S</b>	E	L	Y	H	R	R	N	L	I	G
JAK2	Y	L	P	Y	G	<b>S</b>	D	L	Y	H	R	R	N	L	I	G
TKY2	Y	V	P	L	G	<b>S</b>	D	L	Y	H	R	R	N	L	I	G

Given that the four JAKs share 50–60% sequence identity over the entire kinase domain and more than 80% sequence identity in the catalytic domain, selective targeting of JAK3 with traditional ATP-competitive inhibitors has proven to be difficult [2,6,14]. Tofacitinib, initially described as a selective JAK3 inhibitor, has been approved by the US Food and Drug Administration for the treatment of rheumatoid arthritis [16,17]. However, tofacitinib has recently been verified to be a pan-JAK inhibitor ( $K_i = 0.68, 0.99, 0.24,$  and  $4.39$  nM for JAK1, JAK2, JAK3, and TYK2, respectively), which may lead to undesirable side effects caused by JAK1 and JAK2 inhibition, such as dyslipidemia and suppression of hematopoiesis, respectively [15–20]. Another JAK3 inhibitor, decernotinib, has also been identified as a pan-JAK inhibitor ( $K_i = 11, 13, 2.5,$  and  $13$  nM for JAK1, JAK2, JAK3, and TYK2, respectively) [4]. What this means is that no true JAK3-selective inhibitors have been promoted into clinical trials to date [4,20]. Further improving the understanding of the structure of JAK3, researchers have found that JAK3 has a unique cysteine residue at position 909 (Cys909) in the binding pocket (Table 1). This is different from the other JAKs and could be used to form a covalent interaction with a specific inhibitor to achieve high selectivity [8,10,14]. Employing this mechanism, some irreversible covalent JAK3 inhibitors have been recently published (Fig. 1) [4,11,13,21,22].

Excitingly, most JAK3 covalent inhibitors have been identified as highly potent and selective biochemical and cellular inhibitors of JAK3 [4,11,13,21,22]. Among them, PF-06651600, a true JAK3 inhibitor, exhibits overall properties suitable for both preclinical assessment and advancement to human clinical trials [23]. Bioisosterism, a well-established concept in drug discovery and structure optimization, can be used to improve the potency, selectivity, and physicochemical properties of bioactive compounds [24]. Therefore, we designed and synthesized a novel series of JAK3 irreversible covalent inhibitors by taking tofacitinib as a lead structure: cyclizing (3*R*,4*R*)-(4-methylpiperidin-3-yl)methylamine and replacing it with aniline substituents as linkers in the lipophilic pocket of JAK3; generation of 7*H*-pyrrolo[2,3-*d*]pyrimidine bioisosteres as scaffolds in the hinge region of JAK3; and extending side chains with more electrophilic warheads to form covalent bonds with

Cys909 in JAK3 (Fig. 2). Furthermore, the results from kinase assays for all the synthesized compounds showed a clear structure–activity relationship (SAR). The representative compound **T29** displayed the best enzymatic potency and kinase selectivity not only among all the synthesized compounds in this study, but also among the examples in Fig. 1.

## Results and discussion

### Chemistry and kinase inhibition assays

To investigate the SAR (scaffolds, linkers, and electrophilic warheads) of these designed JAK3 covalent inhibitors, different synthetic approaches and protective group strategies were necessary. At the beginning of our research, compounds **T1–T14**, derived from the purine scaffold, were prepared through the five steps as shown in Scheme 1. The common reagent 6-chloropurine (**1**) was protected with a tetrahydropyran (THP) group to produce adduct**2**, whose improved solubility allowed further coupling. 6-Phenyl-substituted purine derivatives **3-1** and **3-2** were obtained via Suzuki coupling by reacting the adduct with (3-nitrophenyl)boronic acid and (4-methyl-3-nitrophenyl)boronic acid, respectively. Reduction of the nitro group using Pd/C and ammonium formate gave the respective key anilines intermediates **4-1** and **4-2**. Several kinds of electrophilic warheads were introduced into the anilines, and subsequently target compounds **T1–T14** were obtained by removing the protecting groups in acidic conditions.

The inhibitory activities of the prepared compounds were first evaluated against JAK3 kinase in vitro at 0.5 and 5  $\mu$ M in the presence of  $K_m$  ATP. Compounds that inhibited JAK3 over 50% at 0.5  $\mu$ M were further tested to determine their  $IC_{50}$  values for JAK3 and inhibition rates for other JAKs at 0.5 and 5  $\mu$ M (Sup. Table S1). The enzymatic potencies of compounds **T1–T14** are summarized in Table 2. Compounds with acrylamide (**T1**, **T8**) and  $\alpha$ -haloketones (**T5**, **T6**, **T12**, **T13**) as electrophilic warheads selectively inhibited JAK3 at low nanomolar concentrations but did not inhibit other JAKs ( $IC_{50} > 0.5$   $\mu$ M), showing that using a covalent interaction with cysteine 909 could lead to inhibitors with high

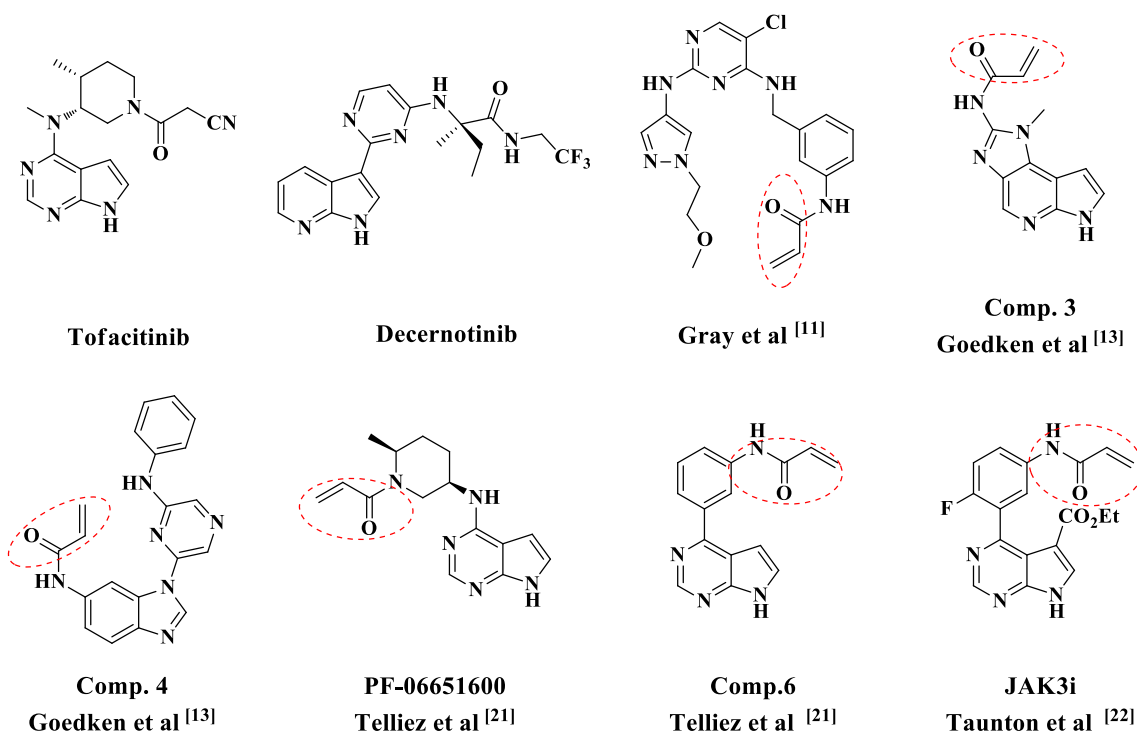


**Fig. 1** Structures of tofacitinib, decernotinib, and reported JAK3 irreversible covalent drugs

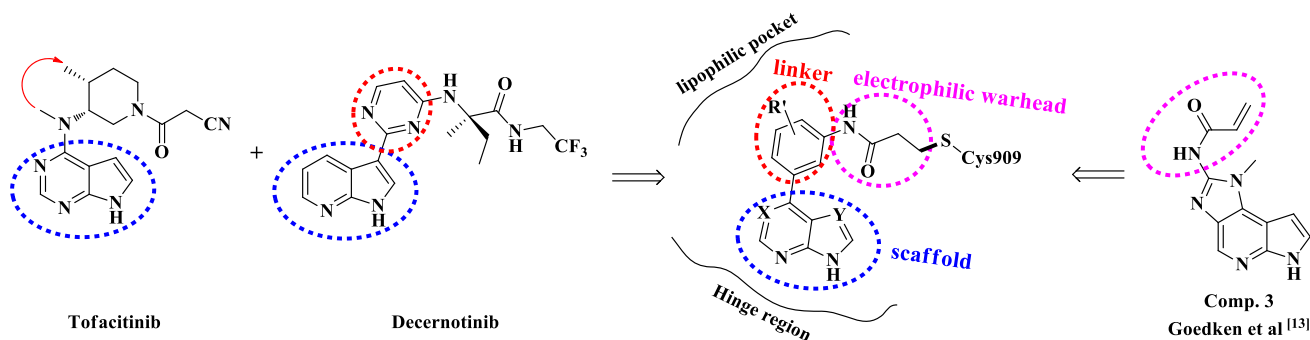
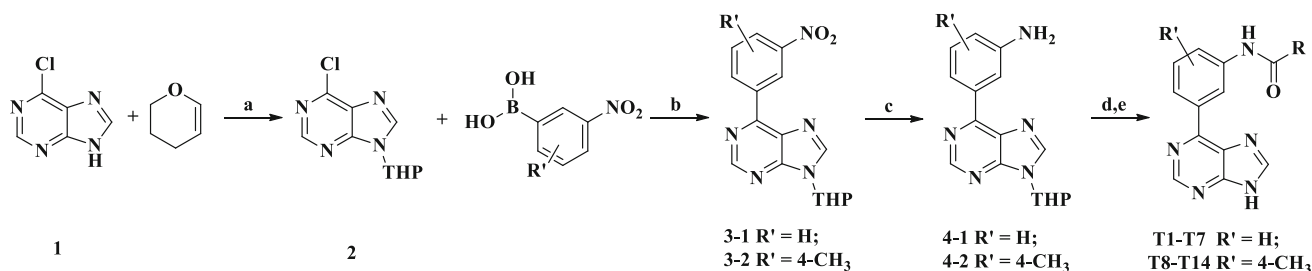


**Fig. 2** Design strategy for JAK3 covalent compounds

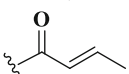
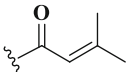
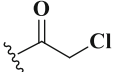
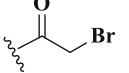
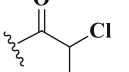
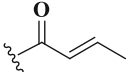
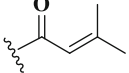
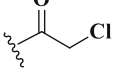
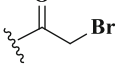
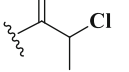


**Scheme 1** General synthesis of purine derivatives **T1–T14**. Reagents and conditions: **a** TsOH, AcOEt, reflux, 2 h; **b** Pd(dppf)Cl<sub>2</sub>, K<sub>2</sub>CO<sub>3</sub>, PhMe/EtOH, reflux, 3–4 h; **c** Pd/C, NH<sub>4</sub>COOH, MeOH, reflux, 2 h; **d** DIEA, dry DMF, r.t., overnight; **e** HCl in dioxane, MeOH, reflux, 1 h

JAK3 selectivity versus other JAKs. Unfortunately, modifications of acrylamide or  $\alpha$ -haloketones (eg., **T2**, **T7**, **T9**, **T14**) resulted in a dramatic loss of inhibitory activity, probably because of the substituents blocking the electrophilic

warheads from forming a covalent bond with cysteine. Modifying the phenyl group with R' substituents led to no obvious influence on inhibitory activity against JAKs, as shown by comparing **T1** with **T8**, **T5** with **T12**, and **T6** with **T13**.

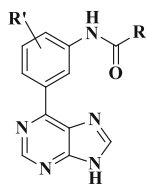
**Table 2** Structures and enzyme potencies of compounds **T1–T14**<sup>a,b</sup>

Comp.	R'	R	JAK1 IC <sub>50</sub> <sup>a</sup> (μM)	JAK2 IC <sub>50</sub> <sup>a</sup> (μM)	JAK3 IC <sub>50</sub> <sup>b</sup>	TYK2 IC <sub>50</sub> <sup>a</sup> (μM)
T1	–		> 5	> 5	2.6 ± 0.13 nM	> 5
T2	–		> 5	> 5	496 ± 2.21 nM	> 5
T3	–		NT	NT	> 5 μM	NT
T4	–		NT	NT	> 5 μM	NT
T5	–		> 5	> 5	2.6 ± 0.09 nM	> 5
T6	–		> 5	> 0.5	2.3 ± 0.11 nM	> 5
T7	–		NT	NT	> 0.5 μM	NT
T8	4-CH <sub>3</sub>		> 5	> 5	3.6 ± 0.07 nM	> 5
T9	4-CH <sub>3</sub>		NT	NT	> 0.5 μM	NT
T10	4-CH <sub>3</sub>		NT	NT	> 5 μM	NT
T11	4-CH <sub>3</sub>		NT	NT	> 5 μM	NT
T12	4-CH <sub>3</sub>		> 5	> 5	2.5 ± 0.10 nM	> 5
T13	4-CH <sub>3</sub>		> 5	> 5	2.5 ± 0.15 nM	> 5
T14	4-CH <sub>3</sub>		NT	NT	> 0.5 μM	NT

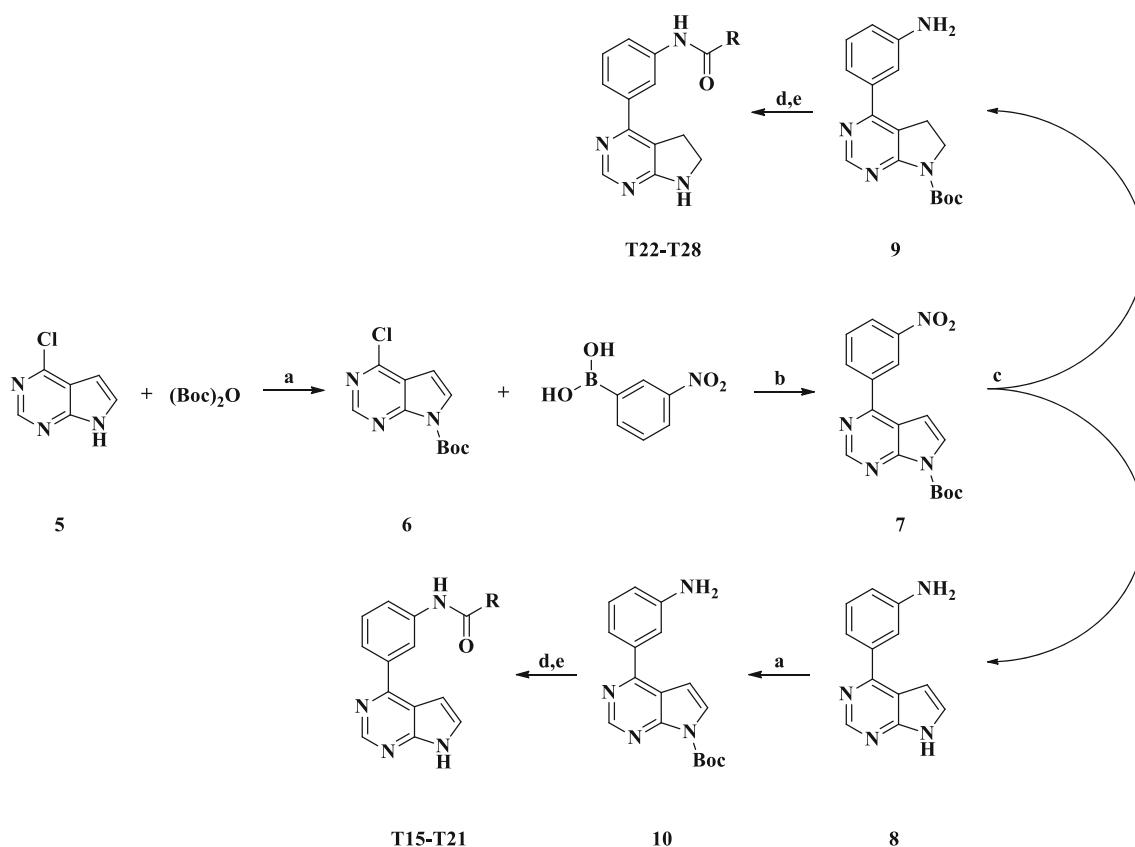
NT not tested

<sup>a</sup>Compounds were measured at concentrations of 5 and 0.5 μM with *K<sub>m</sub>*ATP (30 nM JAK1 and 90 μM ATP; 2 nM JAK2 and 20 μM ATP; 15 nM TYK2 and 16 μM ATP). Mean ± standard error of the mean (SEM), *n* = 2

<sup>b</sup>IC<sub>50</sub> values for JAK3 were an average of at least two independent dose–response curves at *K<sub>m</sub>*ATP (4 nM JAK3 and 6.2 μM ATP)



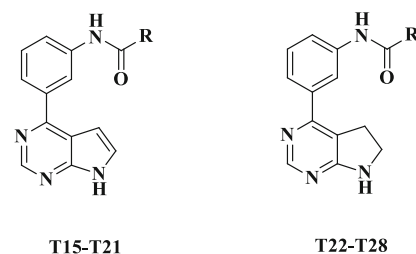
Based on the above results, we selected meta-nitroaniline as the linker and focused on the study of a scaffold. Compounds derived from 7*H*-pyrrolo[2,3-*d*]pyrimidine, a bioisostere of purine and pharmacophore of tofacitinib, were prepared as described in Scheme 2. 4-Chloro-7*H*-



**Scheme 2** General synthesis of pyrrolo[2,3-*d*]pyrimidine derivatives **T15–T28**. Reagents and conditions: **a** DMAP, THF, r.t., 0.5 h; **b** Pd(dppf)Cl<sub>2</sub>, K<sub>2</sub>CO<sub>3</sub>, PhMe/EtOH, reflux, 3–4 h; **c** Pd/C, NH<sub>4</sub>COOH, MeOH, reflux, 2 h; **d** DIEA, dry DMF, r.t., overnight; **e** HCl in dioxane, MeOH, reflux, 1 h

pyrrolo[2,3-*d*]pyrimidine (**5**) reacted with di-*t*-butyl dicarbonate to produce Boc-protected intermediate **6**, which was then coupled with nitrophenylboronic acid to obtain compound **7**. Reduction of the nitro group with Pd/C gave two products, **8** and **9**, and the former was protected again with a Boc group. Final compounds **T15–T28** were obtained by introducing electrophilic warheads to the corresponding key intermediates **10** and **9**, and removing protecting groups.

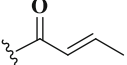
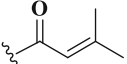
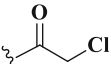
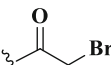
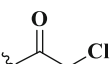
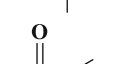
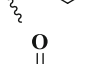
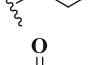
As expected, acrylamide (**T15** and **T22**) and  $\alpha$ -haloketones (**T19**, **T20**, **T26**, and **T27**) analogues retained excellent inhibitory activities against JAK3 (Table 3). In comparison with the corresponding purine derivatives, 7*H*-pyrrolo[2,3-*d*]pyrimidine derivatives significantly increased the inhibitory potency, while 6,7-dihydro-5*H*-pyrrolo[2,3-*d*]pyrimidine derivatives slightly decreased potency. It is worth mentioning that compounds **T15**, **T16**, **T19**, and **T20** notably inhibited JAK2, (> 70% at 5  $\mu$ M, see Sup. Table S1), which has the highest homology to JAK3 [2,6,14]. The results above suggest that compounds bearing a 7*H*-pyrrolo[2,3-*d*]pyrimidine scaffold increase the inhibition of JAK3, as well as JAK2.



Ultimately, compounds **T29–T33**, which are based on the 1*H*-pyrrolo[2,3-*b*]pyridine scaffold, another bioisostere of purine and the core of decernotinib, were synthesized as illustrated in Scheme 3. Removal of the tosyl protecting group in compound **11** and **14** was achieved under alkaline conditions, while the other reactions were similar to those shown in Scheme 2.

Surprisingly, both compounds **T30** and **T33** inhibited JAK3 over 50% at 0.5  $\mu$ M (Sup. Table S1), and their IC<sub>50</sub> values were also more potent than 100 nM (Table 4). The other three compounds (**T29**, **T31**, and **T32**) exhibited better inhibition of JAK3 than any other cores with the corresponding electrophilic warheads. More importantly, those 1*H*-pyrrolo[2,3-*b*]pyridine analogues all could not efficaciously inhibit JAK2, with IC<sub>50</sub> values greater than 5  $\mu$ M. Taken

**Table 3** Structures and enzyme potencies of compounds **T15–T28**<sup>a,b</sup>

Comp.	R	JAK1 IC <sub>50</sub> <sup>a</sup> (μM)	JAK2 IC <sub>50</sub> <sup>a</sup> (μM)	JAK3 IC <sub>50</sub> <sup>b</sup>	TYK2 IC <sub>50</sub> <sup>a</sup> (μM)
T15 [21]		> 5	> 0.5	0.77 ± 0.04 nM	> 5
T16		> 5	> 0.5	23 ± 0.11 nM	> 5
T17		NT	NT	> 0.5 μM	NT
T18		NT	NT	> 5 μM	NT
T19		> 5	> 0.5	1.02 ± 0.02 nM	> 5
T20		> 5	> 0.5	0.93 ± 0.01 nM	> 5
T21		NT	NT	> 0.5 μM	NT
T22		> 5	> 5	3.5 ± 0.09 nM	> 5
T23		> 5	> 5	> 0.5 μM	> 5
T24		NT	NT	> 5 μM	NT
T25		NT	NT	> 5 μM	NT
T26		> 5	> 5	2.7 ± 0.10 nM	> 5
T27		> 5	> 5	2.5 ± 0.21 nM	> 5
T28		NT	NT	> 0.5 μM	NT

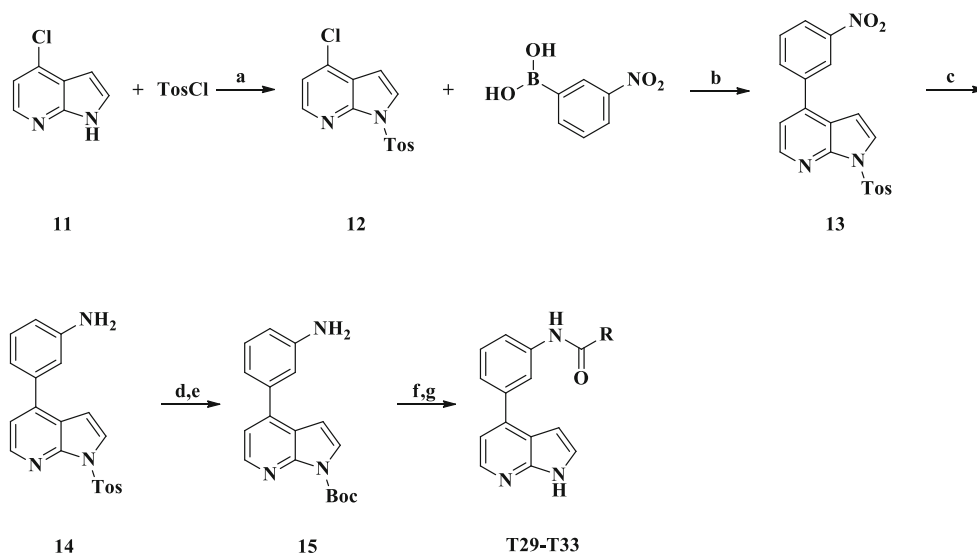
NT not tested

<sup>a</sup>Compounds were measured at concentrations of 5 and 0.5 μM with *K<sub>m</sub>*ATP (30 nM JAK1 and 90 μM ATP; 2 nM JAK2 and 20 μM ATP; 15 nM TYK2 and 16 μM ATP). Mean ± standard error of the mean (SEM), *n* = 2

<sup>b</sup> IC<sub>50</sub> values of JAK3 were an average of at least two independent dose–response curves at *K<sub>m</sub>*ATP (4 nM JAK3 and 6.2 μM ATP)

together, these results suggest that compounds derived from the 1*H*-pyrrolo[2,3-*b*]pyridine pharmacophore possessed favorable inhibition potencies for JAK3 and high selectivity over other JAKs. Therefore, the SAR of pyrimidinyl heterocyclic derivatives in suppressing JAK3 can be summa-

rized as follows: For the scaffold, the order of potency was 1*H*-pyrrolo[2,3-*b*]pyridine > 7*H*-pyrrolo[2,3-*d*]pyrimidine > 9*H*-purine > 6,7-dihydro-5*H*-pyrrolo[2,3-*d*]pyrimidine; for the linker, no significant bioactivity changes are observed, whether there were substituents on the phenyl group or



**Scheme 3** General synthesis of 1*H*-pyrrolo[2,3-*b*]pyridine derivatives **T29–T33**. Reagents and conditions: **a** aq NaOH, ACE, r.t., 0.5 h; **b** Pd(dppf)Cl<sub>2</sub>, K<sub>2</sub>CO<sub>3</sub>, PhMe/EtOH, reflux, 3–4 h; **c** Pd/C, NH<sub>4</sub>COOH,

MeOH, reflux, 2 h; **d** MeOH/THF, Cs<sub>2</sub>CO<sub>3</sub>, r.t., overnight; **e** DMAP, THF, r.t., 0.5 h; **f** DIEA, dry DMF, r.t., overnight; **g** HCl in dioxane, MeOH, reflux, 1 h

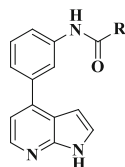
**Table 4** Structures and enzyme potencies of compounds **T29–T33**<sup>a,b</sup>

Comp.	R	JAK1 IC <sub>50</sub> <sup>a</sup> (μM)	JAK2 IC <sub>50</sub> <sup>a</sup> (μM)	JAK3 IC <sub>50</sub> <sup>b</sup> (nM)	TYK2 IC <sub>50</sub> <sup>a</sup> (μM)
T29		> 5	> 5	0.14 ± 0.02	> 5
T30		> 5	> 5	14 ± 0.15	> 5
T31		> 5	> 5	0.21 ± 0.09	> 5
T32		> 5	> 5	0.18 ± 0.09	> 5
T33		> 5	> 5	82 ± 0.03	> 5

<sup>a</sup>Compounds were measured at concentrations of 5 and 0.5 μM with *K<sub>m</sub>*ATP (30 nM JAK1 and 90 μM ATP; 2 nM JAK2 and 20 μM ATP; 15 nM TYK2 and 16 μM ATP). Mean ± standard error of the mean (SEM), *n* = 2

<sup>b</sup>IC<sub>50</sub> values of JAK3 were an average of at least two independent dose–response curves at *K<sub>m</sub>*ATP (4 nM JAK3 and 6.2 μM ATP)

not; for the electrophilic warhead, the order of potency was acrylamide ≈ α-haloketone > methacrylamide > 2-chloropropanamide > (*E*)-but-2-enamide and 3-methylbut-2-enamide.



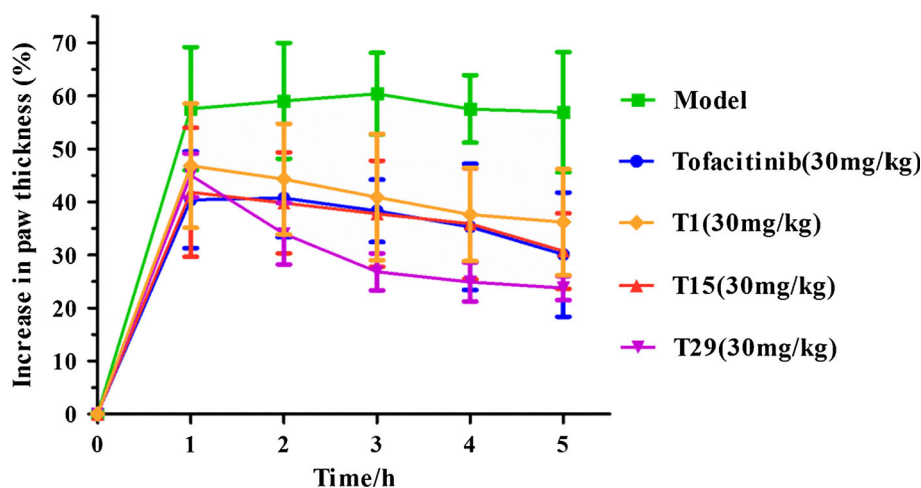
### Cys kinase profiling for selected compounds

JAK3 inhibitors **T1**, **T15**, and **T29** were selected to conduct further investigations for kinase selectivity on the basis of their structure features, bioisosteric scaffolds, and classical electrophilic warhead (acrylamide). Given that these compounds were designed to form covalent bonds with Cys909 in JAK3, kinase selectivity assays were carried out for another nine protein kinases containing a cysteine in the residue analogous to Cys909 in JAK3 (Blk, Bmx, Btk, EGFR,

**Table 5** Cys kinome profiling for select compounds ( $IC_{50}/nM$ )<sup>a,b</sup>

Comp.	JAK3	Blk	Btk <sup>a</sup>	Bmx	EGFR <sup>a</sup>	HER2 <sup>a</sup>	HER4 <sup>a</sup>	Itk	Tec	Rlk
T1	0.0026	> 1 <sup>a</sup>	> 1	0.105 <sup>b</sup>	> 1	> 1	> 1	> 1 <sup>a</sup>	0.454 <sup>b</sup>	> 1 <sup>a</sup>
T15	0.00077	0.911 <sup>b</sup>	> 1	0.024 <sup>b</sup>	> 1	> 1	> 1	0.890 <sup>b</sup>	0.640 <sup>b</sup>	1.000 <sup>b</sup>
T29	0.00014	> 1 <sup>a</sup>	> 1	0.240 <sup>b</sup>	> 1	> 1	> 1	> 1 <sup>a</sup>	0.466 <sup>b</sup>	> 1 <sup>a</sup>

<sup>a</sup>Each enzymatic assay was performed in the presence of an ATP concentration at or close to the  $K_m$  for ATP  
<sup>b</sup> $IC_{50}$  values were an average of two independent dose–response curves

**Fig. 3** Inhibition of carrageenan-induced paw edema in ICR mice. Results are expressed as the mean  $\pm$  SD ( $n = 6$ )

HER2, HER4, Itk, Rlk, Tec, see Sup. Table S2) [14,25]. As summarized in Table 5, compounds **T1** and **T29** could not potently inhibit enzymes that may be good targets for oncology (EGFR, HER2, Blk) and immunological diseases (Btk, Itk), with  $IC_{50}$  values greater than  $1 \mu M$  (Sup. Table S3). Although both compounds displayed similar inhibitory activities against Bmx and Tec, **T29** possessed higher selectivity for JAK3 (over 1700-fold) compared to **T1** (over 40-fold). Compound **T15** inhibited more than half of the kinases of the Cys kinome, especially Bmx, whose  $IC_{50}$  value was only 31-fold that for JAK3. Among these synthesized compounds, **T29** proved to be the optimal compound that possessed not only the best inhibitory activity against JAK3, but also the highest selectivity for other JAKs and kinases belonging to the Cys kinome.

### Evaluation of anti-inflammatory activity in ICR mice

Edema is an important and effective symptom of acute inflammation used to evaluate potential compounds with anti-inflammatory activities. In a carrageenan-induced paw edema test (Fig. 3), the inflammatory response was quantified by measuring the increase in paw size after carrageenan was injected. The paw size in model group mice quickly increased after injecting carrageenan and achieved a maximum at 3 h. Following the oral administration of JAK3 inhibitors (dose: 30 mg/kg, 1 h), paw size began to decrease, in contrast to model mice. Consistent with the order of enzyme inhibi-

tion potency, **T29** showed the best ability to inhibit increased paw thickness, showing a 23.78% ( $p < 0.001$ ) paw size increase at the endpoint. **T1** showed the worst inhibition of edema formation with 36.21%, while **T15** and the positive control tofacitinib displayed 30.78% ( $p < 0.01$ ) and 30.11% ( $p < 0.01$ ), respectively. Therefore, **T29** is the most promising compound of the series with good anti-inflammatory activity in vivo.

### Covalent docking for selected compounds

To better understand the interaction models for selected compounds in the JAK3 active site, we performed covalent in silico docking of the inhibitors in the JAK3 kinase domain. In the modeling of **T29** bound to JAK3 (Fig. 4a), the acrylamide moiety of **T29** was found to form a clear covalent bond with the sulfur atom in Cys909 of JAK3 as expected, which is thought to make **T29** highly selective against other JAKs. In addition, **T29** can also form two hydrogen bonds with Glu903 and Leu905 in the hinge region. Similar results were observed in Fig. 4b, and the overlay of selected inhibitors **T1**, **T15**, and **T29** covalently docked into JAK3 in the same manner. Additionally, in the further analysis of the interaction between JAK3 and **T29**, we found that **T29** extended into or near the protein's hydrophobic region, possibly making hydrophobic interactions with Ala853, Met902, Leu905, Val884, and Leu828 residues (Fig. 4c). Consistent with the order of inhibition potency, the hydrophobicity of scaffold

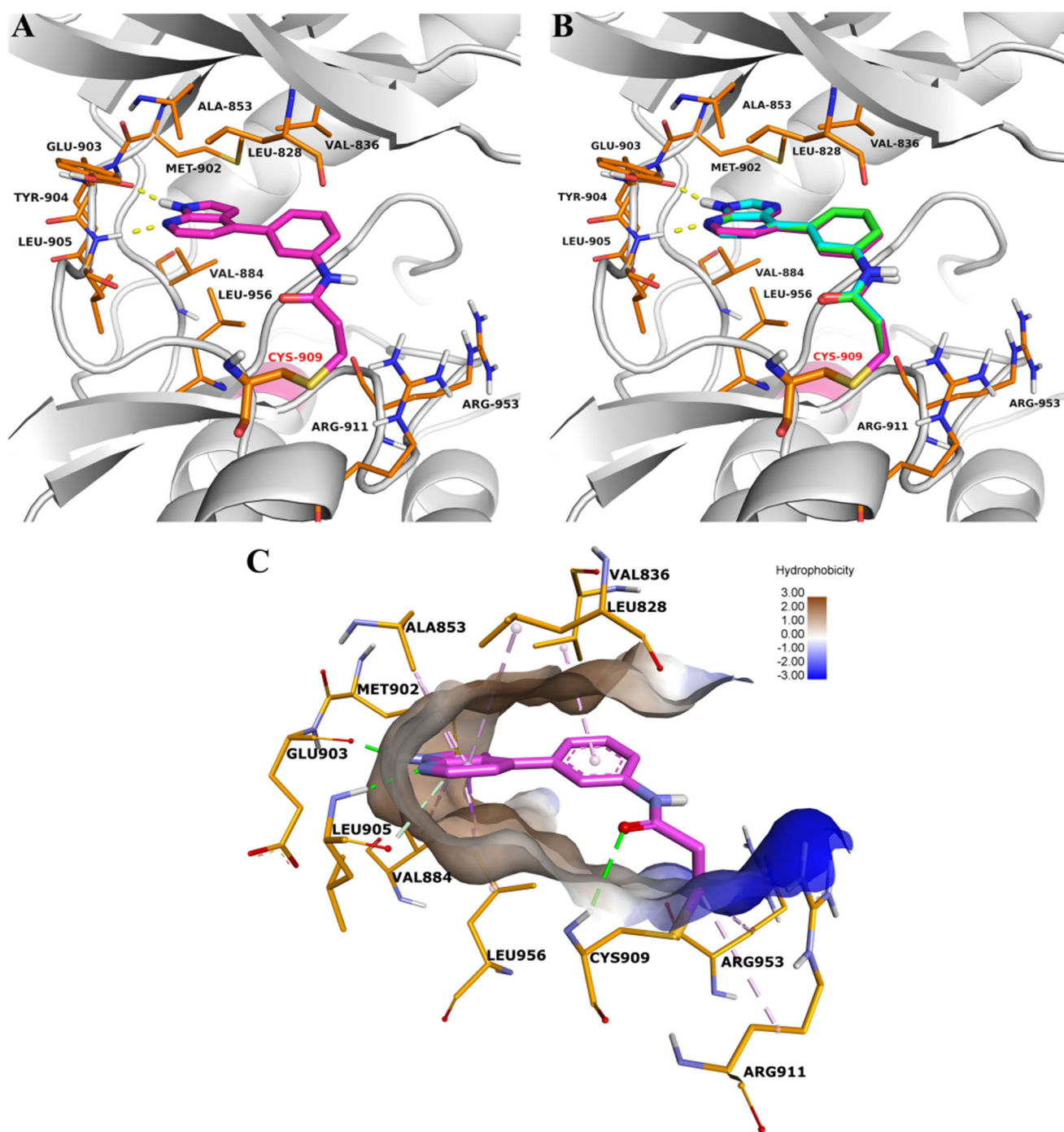


**Fig. 4** Top view of selected compounds (**T1**, **T15**, and **T29**) binding in the JAK3 kinase domain. **a** Compound **T29** covalently docked into JAK3. **b** Overlay of selected compounds covalently docked into JAK3

(**T1**: cyan; **T15**: green; **T29**: magenta). **c** **T29** covalently docked into JAK3, and analysis of the hydrophobic interaction

1*H*-pyrrolo[2,3-*b*]pyridine (**T29**) is higher than that of 7*H*-pyrrolo[2,3-*d*]pyrimidine (**T15**), while 9*H*-purine (**T1**) has a hydrophilic structure, explaining why **T29** achieves a higher degree of efficacy in inactivating JAK3 than **T15** or **T1**. The same explanation applies to other compounds with the same electrophilic warhead and different scaffolds, such as **T2**, **T16**, and **T30**.

### Reversibility of T29 binding

To confirm that the optimal compound **T29** was an irreversible inhibitor, jump dilution analysis [13,26] was used to monitor the conversion of active JAK3 after it was pre-incubated with the inhibitor and the equilibrium was subsequently shifted by dilution to a state favoring inhibitor

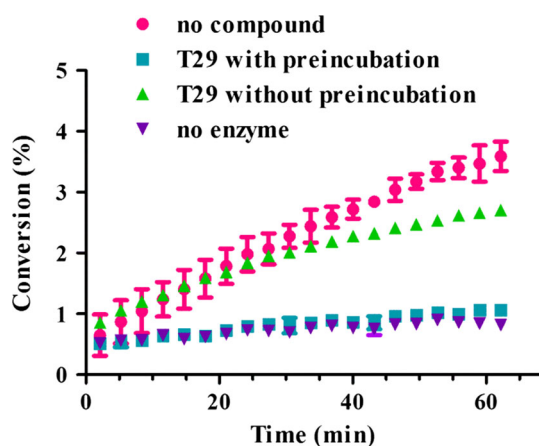


**Fig. 5** **T29** irreversibly inhibited JAK3. **T29** with pre-incubation: compound **T29** was pre-incubated with AK3 for 30 min in the absence of ATP, then diluted with kinase buffer that contains peptide substrate, ATP, and cofactors to the final concentration for reaction, and conversion data were read on a caliper 20 times for 1 h

release. As displayed in Fig. 5, no active JAK3 was detected after it was pre-incubated with **T29** at each time point, identical to the situation in which there is essentially no enzyme, suggesting that JAK3 was completely inhibited by **T29**. Without being pre-incubated with **T29**, JAK3 was observed to be active with a similar increasing trend to conversion with no inhibitor compound. Taken together, **T29** was identified as an irreversible inhibitor.

## Conclusion

In this study, we have described the identification and characterization of a novel series of JAK3 inhibitors with different bioisosteric scaffolds and electrophilic warheads. Biological evaluation of these compounds confirmed that they were selective JAK3 inhibitors; this finding, together with the covalent docking results, revealed a clear SAR. Among the compounds, **T29** proved to be a promising irreversible covalent JAK3 inhibitor that not only possessed the highest potency of inhibition for JAK3 and selectivity against JAKs and kinases containing a cysteine in the residue analogous to Cys909 in JAK3, but also showed significant anti-inflammatory activity in ICR mice by inhibiting the increase in paw thickness. In conclusion, as a potent and selective JAK3 inhibitor, **T29** has the potential to be an efficacious treatment for inflammatory diseases and is worth further optimizing to improve its potency and medicinal properties.

## Experimental section

**Chemistry** Chemistry reagents of analytical grade were purchased from Changzheng Chemical Factory, Chengdu,

Sichuan, P.R. China, and they were directly used without any purification. TLC was performed on 0.20 mm Silica gel 60 F<sub>254</sub> plates (Qingdao Ocean Chemical Factory, Shandong, China). Hydrogen nuclear magnetic resonance (<sup>1</sup>H NMR) spectra were recorded at 400 MHz while carbon nuclear magnetic resonance (<sup>13</sup>C NMR) spectra were recorded at 101 MHz on a Varian spectrometer (Varian, Palo Alto, CA) model Gemini 400 and reported in parts per million. Chemical shifts ( $\delta$ ) are quoted in ppm relative to tetramethylsilane (TMS) as an internal standard, where ( $\delta$ ) TMS = 0.00 ppm. The multiplicity of the signal is indicated as s, singlet; brs, broad singlet; d, doublet; t, triplet; q, quartet; m, multiplet, defined as all multiplex signals where overlap or complex coupling of signals makes definitive descriptions of peaks difficult. High-resolution mass spectra (HRMS) were measured by MALDI Q-ToF Premier mass spectrometer (Micromass, Manchester, UK). Room temperature is within the range 20–25 °C. The purity was analyzed by HPLC system (Waters 2695, separations module) with a photodiode array detector (Waters 2996, Milford, MA, USA), and the chromatographic column was a reversed phase C18 column (Waters, 150 mm  $\times$  4.6 mm, i.d. 5  $\mu$ m). All compounds were supplied in HPLC degree methanol with 10  $\mu$ L, which was injected into a partial loop, with isocratic elution with 70% methanol and 30% water at a flow rate of 1 mL/min. The purity of all tested compounds was  $\geq$  95% according to our analytical HPLC method.

## General procedure for the preparation of compound 2

A suspension of 6-chloro-9H-purine (**1**, 7.73 g, 50 mmol) and 4-methylbenzenesulfonic acid (130 mg, 0.75 mmol) in EtOAc (100 mL) was treated with 3,4-dihydro-2H-pyran (5.05 g, 60 mmol). The mixture was stirring and heating at 90 °C, then the solid slowly dissolved over 2 h. The flask was removed from the oil bath and the cloudy yellow reaction mixture was filtered, the filtrate extracted with water and brine in sequence, and the combined organic layers were dried over anhydrous Na<sub>2</sub>SO<sub>4</sub>. The organic layer was concentrated in vacuo to afford desired product as yellow oil in a good yield of 92.3% (11.02 g). <sup>1</sup>H NMR (400 MHz, CDCl<sub>3</sub> - d<sub>1</sub>) $\delta$ : 8.69 (s, 1H), 8.28 (s, 1H), 5.73 (dd,  $J$  = 10.4, 2.3 Hz, 1H), 4.16–4.09 (m, 1H), 3.73 (td,  $J$  = 11.6, 2.8 Hz, 1H), 2.11 (d,  $J$  = 10.8 Hz, 1H), 2.06–1.96 (m, 2H), 1.78–1.67 (m, 2H), 1.62 (d,  $J$  = 8.0 Hz, 1H).

## General procedure for the preparation of compounds 6 and 10

A mixture of **5** or **9** (1 eq) in THF was added DMAP (0.02 eq) and di-*tert*-butyl dicarbonate (1.1 eq) in sequence. The reaction mixture was continued to stir at ambient temperature for about 1 h and then evaporated in vacuo. The residue was diluted with water and extracted with EtOAc. The combined

organic layers were washed with brine, dried over anhydrous  $\text{Na}_2\text{SO}_4$ , and evaporated in vacuo. The crude product was used in the next procedure without further purification.

*Tert*-butyl 4-chloro-7*H*-pyrrolo[2,3-*d*]pyrimidine-7-carboxylate (**6**). White solid. Yield 94.8%.  $^1\text{H}$  NMR (400 MHz,  $\text{CDCl}_3$ - $d_1$ ) $\delta$ : 8.78 (s, 1H), 7.64 (d,  $J = 4.1$  Hz, 1H), 6.60 (d,  $J = 4.1$  Hz, 1H), 1.62 (s, 9H).

*Tert*-butyl 4-(3-aminophenyl)-7*H*-pyrrolo[2,3-*d*]pyrimidine-7-carboxylate (**10**). White solid. Yield 72.3%.  $^1\text{H}$  NMR (400 MHz,  $\text{DMSO}-d_6$ ) $\delta$ : 8.99 (s, 1H), 7.92 (d,  $J = 4.1$  Hz, 1H), 7.36 (s, 1H), 7.23 (d,  $J = 4.9$  Hz, 2H), 7.04 (d,  $J = 4.1$  Hz, 1H), 6.75 (dd,  $J = 7.3, 3.8$  Hz, 1H), 5.39 (s, 2H), 1.64 (s, 9H).

### General procedure for the preparation of compound 12

At about 0 °C, NaOH (2 mol/L in water, 4.8 g, 120 mmol) was added to a solution of 4-chloro-1*H*-pyrrolo[2,3-*b*]pyridine (15.2 g, 100 mmol) and 4-methylbenzene-1-sulfonyl chloride (19.95 g, 105 mmol) in acetone. The resulting solution was stirred at ambient temperature for about 6 h. The solids were collected by filtration and washed with acetone/water to give the title product as white solid in a yield of 88.1% (26.92 g).  $^1\text{H}$  NMR (400 MHz,  $\text{DMSO}-d_6$ )  $\delta$ : 8.35 (d,  $J = 5.2$  Hz, 1H), 8.04 (d,  $J = 4.0$  Hz, 1H), 8.01 (d,  $J = 8.1$  Hz, 2H), 7.47 (d,  $J = 5.2$  Hz, 1H), 7.43 (d,  $J = 8.1$  Hz, 2H), 6.88 (d,  $J = 4.0$  Hz, 1H), 2.35 (s, 3H).

### General procedure of Suzuki coupling for the preparation of compounds 3, 7, and 13

Toluene/EtOH (7/3, v/v) was added to an nitrogen-purged flask containing the halide intermediate (1 eq),  $\text{PdCl}_2(\text{dppf})$  (0.05 eq),  $\text{K}_2\text{CO}_3$  (3 eq), and appropriate boronic acid (1.1 eq), and then the mixture was stirred under nitrogen at 80 °C for 3–4 h. After cooling to ambient temperature, the mixture was filtered with celite and concentrated in vacuo. The residue was dissolved in water, extracted with EtOAc, washed with brine, and dried over anhydrous  $\text{Na}_2\text{SO}_4$ . The organic layer was evaporated in vacuo, and the residue was purified on a silica gel column to give desired product.

6-(3-Nitrophenyl)-9-(tetrahydro-2*H*-pyran-2-yl)-9*H*-purine (**3-1**). Yellow solid. Yield 65.7%.  $^1\text{H}$  NMR (400 MHz,  $\text{CDCl}_3$ - $d_1$ ) $\delta$ : 9.74 (d,  $J = 1.8$  Hz, 1H), 9.22 (d,  $J = 7.9$  Hz, 1H), 9.07 (s, 1H), 8.41 (s, 1H), 8.39–8.35 (m, 1H), 7.75 (t,  $J = 8.0$  Hz, 1H), 5.88 (dd,  $J = 10.3, 2.5$  Hz, 1H), 4.05 (d,  $J = 9.0$  Hz, 1H), 3.74 (td,  $J = 11.3, 4.1$  Hz, 1H), 2.42–2.30 (m, 1H), 2.08–1.97 (m, 2H), 1.84–1.71 (m, 1H), 1.63 (d,  $J = 11.8$  Hz, 2H).

6-(4-Methyl-3-nitrophenyl)-9-(tetrahydro-2*H*-pyran-2-yl)-9*H*-purine (**3-2**). Yellow solid. Yield 63.2%.  $^1\text{H}$  NMR (400 MHz,  $\text{DMSO}-d_6$ ) $\delta$ : 9.47 (d,  $J = 2.0$  Hz, 1H), 9.13 (dd,  $J = 8.6, 2.0$  Hz, 1H), 9.10 (s, 1H), 9.03 (s, 1H), 8.06 (d,  $J = 8.5$  Hz, 1H), 5.87 (d,  $J = 10.9$  Hz, 1H), 4.07 (d,

$J = 11.8$  Hz, 1H), 3.76 (m, 1H), 2.38 (d,  $J = 12.1$  Hz, 1H), 2.31 (s, 3H), 2.03 (t,  $J = 13.7$  Hz, 2H), 1.77 (m, 1H), 1.63 (d,  $J = 11.4$  Hz, 2H).

*Tert*-butyl 4-(3-nitrophenyl)-7*H*-pyrrolo[2,3-*d*]pyrimidine-7-carboxylate (**7**). Yellow solid. Yield 67.7%.  $^1\text{H}$  NMR (400 MHz,  $\text{DMSO}-d_6$ ) $\delta$ : 9.13 (s, 1H), 8.87 (s, 1H), 8.57 (d,  $J = 7.7$  Hz, 1H), 8.44 (d,  $J = 8.1$  Hz, 1H), 8.04 (d,  $J = 4.1$  Hz, 1H), 7.92 (t,  $J = 8.0$  Hz, 1H), 7.19 (d,  $J = 4.1$  Hz, 1H), 1.65 (s, 9H).

4-(3-Nitrophenyl)-7-tosyl-7*H*-pyrrolo[2,3-*d*]pyrimidine (**13**). Yellow solid. Yield 60.8%.  $^1\text{H}$  NMR (400 MHz,  $\text{CDCl}_3$ - $d_1$ ) $\delta$ : 8.56 (s, 1H), 8.46 (s, 1H), 8.32 (d,  $J = 7.8$  Hz, 1H), 8.13 (d,  $J = 7.7$  Hz, 2H), 7.93 (d,  $J = 7.2$  Hz, 1H), 7.85 (d,  $J = 3.7$  Hz, 1H), 7.71 (t,  $J = 7.6$  Hz, 1H), 7.31 (d,  $J = 8.0$  Hz, 3H), 6.73 (d,  $J = 3.7$  Hz, 1H), 2.39 (s, 3H).

### General procedure of nitro reduction for the preparation of compounds 4, 8, 9, and 14

To the Suzuki coupling product (1 eq) and ammonium formate (3 eq) in MeOH was added 10% Pd/C (0.5%w). Then, the mixture was stirred under nitrogen at 80 °C for 2 h. The mixture was filtered with celite and washed with MeOH. The filtrate was concentrated in vacuo. The residue was dissolved in water, extracted with EtOAc, brine, and dried over anhydrous  $\text{Na}_2\text{SO}_4$ . The organic layer was evaporated in vacuo, and the residue was purified on a silica gel column to give the corresponding product.

3-(7-(Tetrahydro-2*H*-pyran-2-yl)-7*H*-pyrrolo[2,3-*d*]pyrimidin-4-yl)aniline (**4-1**). Yellow solid. Yield 62.5%.  $^1\text{H}$  NMR (400 MHz,  $\text{DMSO}-d_6$ ) $\delta$ : 8.95 (s, 1H), 8.84 (s, 1H), 8.06 (s, 1H), 8.04 (d,  $J = 1.1$  Hz, 1H), 7.22 (t,  $J = 7.9$  Hz, 1H), 6.79\*–6.71 (m, 1H), 5.82 (d,  $J = 9.5$  Hz, 1H), 5.32 (s, 2H), 4.05 (d,  $J = 9.0$  Hz, 1H), 3.74 (td,  $J = 11.3, 4.1$  Hz, 1H), 2.42–2.30 (m, 1H), 2.08–1.97 (m, 2H), 1.84–1.71 (m, 1H), 1.63 (d,  $J = 11.8$  Hz, 2H).

6-(4-Methyl-3-nitrophenyl)-9-(tetrahydro-2*H*-pyran-2-yl)-9*H*-purine (**4-2**). Yellow solid. Yield 45.7%.  $^1\text{H}$  NMR (400 MHz,  $\text{DMSO}-d_6$ ) $\delta$ : 8.92 (s, 1H), 8.83 (s, 1H), 8.07 (d,  $J = 8.9$  Hz, 2H), 7.12 (d,  $J = 7.7$  Hz, 1H), 5.81 (d,  $J = 10.6$  Hz, 1H), 5.13 (s, 2H), 4.04 (d,  $J = 11.9$  Hz, 1H), 3.74 (td,  $J = 11.4, 4.3$  Hz, 1H), 2.35 (dd,  $J = 17.6, 6.4$  Hz, 1H), 2.31 (s, 3H), 2.02 (d,  $J = 10.8$  Hz, 2H), 1.77 (m, 1H), 1.63 (d,  $J = 11.5$  Hz, 2H).

3-(7*H*-Pyrrolo[2,3-*d*]pyrimidin-4-yl)aniline (**8**). White solid. Yield 30.1%.  $^1\text{H}$  NMR (400 MHz,  $\text{DMSO}-d_6$ ) $\delta$ : 12.16 (s, 1H), 8.77 (s, 1H), 7.95 (s, 1H), 7.44 (s, 1H), 7.32 (d,  $J = 7.5$  Hz, 1H), 7.20 (t,  $J = 7.7$  Hz, 1H), 6.85 (d,  $J = 2.3$  Hz, 1H), 6.72 (d,  $J = 7.9$  Hz, 1H), 5.29 (s, 2H).

*Tert*-butyl 4-(3-aminophenyl)-5*H*-pyrrolo[2,3-*d*]pyrimidine-7(6*H*)-carboxylate (**9**). White solid. Yield 37.4%.  $^1\text{H}$  NMR (400 MHz,  $\text{DMSO}-d_6$ ) $\delta$ : 8.69 (s, 1H), 7.20 (s, 1H), 7.15 (t,  $J = 7.8$  Hz, 1H), 7.03 (d,  $J = 7.9$  Hz, 1H), 6.67

(d,  $J = 7.4$  Hz, 1H), 5.29 (s, 2H), 3.95 (t,  $J = 8.4$  Hz, 2H), 3.28 (t,  $J = 8.4$  Hz, 2H), 1.51 (s, 9H).

3-(7-Tosyl-7*H*-pyrrolo[2,3-*d*]pyrimidin-4-yl)aniline (**14**). White solid. Yield 56.9%.  $^1\text{H NMR}$  (400 MHz,  $\text{CDCl}_3 - d_1$ ) $\delta$ : 8.44 (d,  $J = 4.9$  Hz, 1H), 8.10 (d,  $J = 8.1$  Hz, 2H), 7.74 (d,  $J = 3.9$  Hz, 1H), 7.29 (s, 3H), 7.20 (d,  $J = 4.8$  Hz, 1H), 7.00 (d,  $J = 7.5$  Hz, 1H), 6.93 (s, 1H), 6.81 (d,  $J = 7.9$  Hz, 1H), 6.78 (d,  $J = 3.9$  Hz, 1H), 2.37 (s, 3H).

#### General Procedure for the preparation of compound 15

A solution of **14** (1.09 g, 3 mmol) in MeOH/THF (3/1, v/v, 26 mL) was added  $\text{Cs}_2\text{CO}_3$  (1.47 g, 4.5 mmol) under stirring at ambient temperature, and then the reaction mixture was stirred overnight. The solvent was removed by evaporation. The residue was diluted with water and extracted with EtOAc. The combined organic layers were washed with brine, dried over anhydrous  $\text{Na}_2\text{SO}_4$ , and evaporated in vacuo. The crude intermediate was directly used to react with di-*tert*-butyl dicarbonate, just like the preparation for compound **6**, and ultimately giving target compound **15** as white solid in a yield of 40.5% (375.7 mg).  $^1\text{H NMR}$  (400 MHz,  $\text{DMSO}-d_6$ ) $\delta$ : 8.44 (d,  $J = 4.9$  Hz, 1H), 7.74 (d,  $J = 3.9$  Hz, 1H), 7.29 (s, 1H), 7.20 (d,  $J = 4.8$  Hz, 1H), 7.00 (d,  $J = 7.5$  Hz, 1H), 6.93 (s, 1H), 6.81 (d,  $J = 7.9$  Hz, 1H), 6.78 (d,  $J = 3.9$  Hz, 1H), 1.64 (s, 9H).

#### General Procedure for the preparation of compounds T1–T33

A solution of amino intermediate (1 eq) and DIEA (3 eq) in anhydrous DMF was added dropwise to acyl chloride derivative (1.2 eq) under stirring at ambient temperature, and then the reaction mixture was stirred overnight. The reaction mixture was quenched with water and extracted with EtOAc. The organic extract was washed with water and brine, dried over anhydrous  $\text{Na}_2\text{SO}_4$ . The solvent was removed in vacuo to yield the crude product for the next step without further purification.

#### General procedure for THP-deprotection and Boc-deprotection

4M HCl in 1,4-dioxane (3 eq) was added to a stirred solution of appropriate intermediate (1 eq) in MeOH at ambient temperature. The resulting solution was heated to 75 °C under stirring for about 1 h, and the solvent was removed under reduced pressure. The residue was dissolved in water and slowly basified with 10% NaOH solution to pH = 7, then extracted with EtOAc, washed with water and brine, and dried with anhydrous  $\text{Na}_2\text{SO}_4$ . The solvent was removed in vacuo, and the crude product was purified by silica gel column to give target compound.

*N*-(3-(9*H*-Purin-6-yl)phenyl)acrylamide (**T1**). White solid. HPLC purity 97.8%. Yield 42.8%.  $^1\text{H NMR}$  (400 MHz,  $\text{DMSO}-d_6$ ) $\delta$ : 10.49 (s, 1H), 8.99 (s, 2H), 8.71 (s, 1H), 8.58 (d,  $J = 6.7$  Hz, 1H), 8.00 (d,  $J = 7.3$  Hz, 1H), 7.56 (t,  $J = 7.7$  Hz, 1H), 6.53 (dd,  $J = 16.4, 9.8$  Hz, 1H), 6.31 (d,  $J = 16.7$  Hz, 1H), 5.79 (d,  $J = 9.9$  Hz, 1H).  $^{13}\text{C NMR}$  (101 MHz,  $\text{DMSO}-d_6$ )  $\delta$ : 163.84, 154.59, 151.77, 146.21, 139.93, 135.66, 132.35, 129.60, 127.49, 125.33, 122.59, 120.59. HRMS (ESI),  $m/z$ : 266.1034 [ $\text{M} + \text{H}$ ] $^+$ .

*N*-(3-(9*H*-Purin-6-yl)phenyl)methacrylamide (**T2**). White solid. HPLC purity 98.3%. Yield 42.2%.  $^1\text{H NMR}$  (400 MHz,  $\text{DMSO}-d_6$ ) $\delta$ : 10.07 (s, 1H), 9.01 (s, 1H), 8.99 (s, 1H), 8.72 (s, 1H), 8.59 (d,  $J = 7.6$  Hz, 1H), 7.92 (d,  $J = 8.0$  Hz, 1H), 7.55 (t,  $J = 7.9$  Hz, 1H), 5.90 (s, 1H), 5.56 (s, 1H), 1.99 (s, 3H). HRMS (ESI),  $m/z$ : 302.1019 [ $\text{M} + \text{Na}$ ] $^+$ .

(*E*)-*N*-(3-(9*H*-Purin-6-yl)phenyl)but-2-enamide (**T3**). White solid. HPLC purity 98.6%. Yield 38.6%.  $^1\text{H NMR}$  (400 MHz,  $\text{DMSO}-d_6$ ) $\delta$ : 10.24 (s, 1H), 8.93 (s, 1H), 8.89 (s, 1H), 8.67 (s, 1H), 8.47 (d,  $J = 7.5$  Hz, 1H), 7.91 (d,  $J = 7.7$  Hz, 1H), 7.48 (t,  $J = 7.8$  Hz, 1H), 6.78 (dd,  $J = 14.9, 6.9$  Hz, 1H), 6.16 (d,  $J = 15.1$  Hz, 1H), 1.83 (d,  $J = 6.5$  Hz, 3H). HRMS (ESI),  $m/z$ : 302.1013 [ $\text{M} + \text{Na}$ ] $^+$ .

*N*-(3-(9*H*-Purin-6-yl)phenyl)-3-methylbut-2-enamide (**T4**). White solid. HPLC purity 96.2%. Yield 39.7%.  $^1\text{H NMR}$  (400 MHz,  $\text{DMSO}-d_6$ ) $\delta$ : 10.12 (s, 1H), 8.97 (s, 1H), 8.95 (s, 1H), 8.68 (s, 1H), 8.55 (d,  $J = 7.7$  Hz, 1H), 7.91 (d,  $J = 7.6$  Hz, 1H), 7.51 (t,  $J = 7.8$  Hz, 1H), 5.95 (s, 1H), 2.19 (s, 3H), 1.89 (s, 3H). HRMS (ESI),  $m/z$ : 316.1173 [ $\text{M} + \text{Na}$ ] $^+$ .

*N*-(3-(9*H*-Purin-6-yl)phenyl)-2-chloroacetamide (**T5**). White solid. HPLC purity 96.2%. Yield 35.1%.  $^1\text{H NMR}$  (400 MHz,  $\text{DMSO}-d_6$ ) $\delta$ : 13.66 (s, 1H), 10.57 (s, 1H), 8.97 (s, 2H), 8.67 (s, 2H), 7.89 (d,  $J = 8.1$  Hz, 1H), 7.56 (t,  $J = 8.0$  Hz, 1H), 4.31 (s, 2H). HRMS (ESI),  $m/z$ : 310.0473 [ $\text{M} + \text{Na}$ ] $^+$ .

*N*-(3-(9*H*-Purin-6-yl)phenyl)-2-bromoacetamide (**T6**). Light yellow solid. HPLC purity 96.5%. Yield 34.8%.  $^1\text{H NMR}$  (400 MHz,  $\text{DMSO}-d_6$ ) $\delta$ : 10.64 (s, 1H), 9.01 (s, 1H), 8.98 (s, 1H), 8.72 (s, 1H), 8.60 (d,  $J = 7.9$  Hz, 1H), 7.89 (d,  $J = 7.1$  Hz, 1H), 7.56 (d,  $J = 7.1$  Hz, 1H), 4.32 (s, 2H). HRMS (ESI),  $m/z$ : 354.0277 [ $\text{M} + \text{Na}$ ] $^+$ .

*N*-(3-(9*H*-Purin-6-yl)phenyl)-2-chloropropanamide (**T7**). White solid. HPLC purity 97.1%. Yield 35.1%.  $^1\text{H NMR}$  (400 MHz,  $\text{DMSO}-d_6$ ) $\delta$ : 13.66 (s, 1H), 10.59 (s, 1H), 8.98 (d,  $J = 9.1$  Hz, 2H), 8.68 (s, 2H), 7.90 (d,  $J = 8.0$  Hz, 1H), 7.57 (t,  $J = 7.9$  Hz, 1H), 4.75 (dd,  $J = 13.2, 6.6$  Hz, 1H), 1.65 (d,  $J = 6.6$  Hz, 3H). HRMS (ESI),  $m/z$ : 302.0830 [ $\text{M} + \text{H}$ ] $^+$ .

*N*-(2-Methyl-5-(9*H*-purin-6-yl)phenyl)acrylamide (**T8**). White solid. HPLC purity 98.9%. Yield 35.7%.  $^1\text{H NMR}$  (400 MHz,  $\text{DMSO}-d_6$ ) $\delta$ : 9.75 (s, 1H), 8.94 (s, 1H), 8.92 (s, 1H), 8.65 (s, 1H), 8.62 (d,  $J = 8.1$  Hz, 1H), 7.46 (d,

$J = 8.1$  Hz, 1H), 6.59 (dd,  $J = 17.1, 10.5$  Hz, 1H), 6.29 (dd,  $J = 17.0, 2.0$  Hz, 1H), 5.79 (dd,  $J = 10.2, 1.9$  Hz, 1H), 2.31 (s, 3H). HRMS (ESI),  $m/z$ : 302.1017 [M + Na]<sup>+</sup>.

*N*-(2-Methyl-5-(9*H*-purin-6-yl)phenyl)methacrylamide (**T9**). White solid. HPLC purity 98.1%. Yield 36.0%. <sup>1</sup>H NMR (400 MHz, DMSO-*d*<sub>6</sub>) $\delta$ : 9.60 (s, 1H), 8.94 (s, 1H), 8.74 (s, 1H), 8.66 (d,  $J = 6.0$  Hz, 2H), 7.47 (d,  $J = 8.1$  Hz, 1H), 5.92 (s, 1H), 5.54 (s, 2H), 2.28 (s, 3H), 2.00 (s, 3H). HRMS (ESI),  $m/z$ : 332.1417 [M + K]<sup>+</sup>.

(*E*)-*N*-(2-Methyl-5-(9*H*-purin-6-yl)phenyl)but-2-enamide (**T10**). White solid. HPLC purity 97.9%. Yield 33.8%. <sup>1</sup>H NMR (400 MHz, DMSO-*d*<sub>6</sub>) $\delta$ : 9.53 (s, 1H), 8.93 (s, 1H), 8.90 (s, 1H), 8.65 (s, 1H), 8.60 (d,  $J = 7.9$  Hz, 1H), 7.44 (d,  $J = 8.1$  Hz, 1H), 6.85–6.79 (m, 1H), 6.27 (d,  $J = 15.6$  Hz, 2H), 2.30 (s, 3H), 1.89 (d,  $J = 6.8$  Hz, 3H). HRMS (ESI),  $m/z$ : 316.1170 [M + Na]<sup>+</sup>.

3-Methyl-*N*-(2-methyl-5-(9*H*-purin-6-yl)phenyl)but-2-enamide (**T11**). White solid. HPLC purity 98.0%. Yield 33.5%. <sup>1</sup>H NMR (400 MHz, DMSO-*d*<sub>6</sub>) $\delta$ : 9.44 (s, 1H), 8.99 (s, 1H), 8.85 (s, 1H), 8.74 (s, 1H), 8.55 (d,  $J = 7.9$  Hz, 1H), 7.45 (d,  $J = 8.0$  Hz, 1H), 6.04 (s, 1H), 2.31 (s, 3H), 2.17 (s, 3H), 1.89 (s, 3H). HRMS (ESI),  $m/z$ : 330.1387 [M + Na]<sup>+</sup>.

2-Chloro-*N*-(2-methyl-5-(9*H*-purin-6-yl)phenyl)acetamide (**T12**). White solid. HPLC purity 95.7%. Yield 30.0%. <sup>1</sup>H NMR (400 MHz, DMSO-*d*<sub>6</sub>) $\delta$ : 13.63 (s, 1H), 9.89 (s, 1H), 8.92 (s, 1H), 8.88 (s, 1H), 8.69 (d,  $J = 7.9$  Hz, 1H), 8.63 (s, 1H), 7.46 (d,  $J = 8.1$  Hz, 1H), 4.36 (s, 2H), 2.30 (s, 3H). HRMS (ESI),  $m/z$ : 324.0633 [M + Na]<sup>+</sup>.

2-Bromo-*N*-(2-methyl-5-(9*H*-purin-6-yl)phenyl)acetamide (**T13**). White solid. HPLC purity 97.0%. Yield 30.7%. <sup>1</sup>H NMR (400 MHz, DMSO-*d*<sub>6</sub>) $\delta$ : 13.62 (s, 1H), 9.89 (s, 1H), 8.92 (s, 1H), 8.87 (d,  $J = 9.8$  Hz, 1H), 8.69 (d,  $J = 8.2$  Hz, 1H), 8.63 (s, 1H), 7.46 (d,  $J = 8.1$  Hz, 1H), 4.36 (s, 2H), 2.30 (s, 3H). HRMS (ESI),  $m/z$ : 368.0125 [M + Na]<sup>+</sup>.

2-Chloro-*N*-(2-methyl-5-(9*H*-purin-6-yl)phenyl)propanamide (**T14**). White solid. HPLC purity 96.9%. Yield 27.4%. <sup>1</sup>H NMR (400 MHz, DMSO)  $\delta$  13.63 (s, 1H), 9.94 (s, 1H), 8.93 (s, 1H), 8.82 (s, 1H), 8.67 (d,  $J = 22.0$  Hz, 2H), 7.47 (d,  $J = 7.8$  Hz, 1H), 4.82 (q,  $J = 6.6$  Hz, 1H), 2.30 (s, 3H), 1.68 (d,  $J = 6.7$  Hz, 3H). HRMS (ESI),  $m/z$ : 338.0782 [M + Na]<sup>+</sup>.

*N*-(3-(7*H*-pyrrolo[2,3-*d*]pyrimidin-4-yl)phenyl)acrylamide (**T15**). White solid. HPLC purity 99.1%. Yield 32.5%. <sup>1</sup>H NMR (400 MHz, DMSO-*d*<sub>6</sub>) $\delta$ : 12.28 (s, 1H), 10.39 (s, 1H), 8.84 (s, 1H), 8.64 (s, 1H), 7.92 (d,  $J = 7.8$  Hz, 1H), 7.82 (d,  $J = 8.1$  Hz, 1H), 7.75–7.67 (m, 1H), 7.54 (t,  $J = 7.9$  Hz, 1H), 6.96 (dd,  $J = 3.5, 1.7$  Hz, 1H), 6.48 (dd,  $J = 17.0, 10.1$  Hz, 1H), 6.32 (dd,  $J = 17.0, 2.0$  Hz, 1H), 5.80 (dd,  $J = 10.0, 1.9$  Hz, 1H). <sup>13</sup>C NMR (101 MHz, DMSO-*d*<sub>6</sub>) $\delta$ : 164.16, 152.86, 151.83, 146.76, 140.37, 132.22, 130.33, 127.86, 124.58, 123.09, 120.61, 115.06, 102.73. HRMS (ESI),  $m/z$ : 287.0907 [M + Na]<sup>+</sup>.

*N*-(3-(7*H*-Pyrrolo[2,3-*d*]pyrimidin-4-yl)phenyl)methacrylamide (**T16**). White solid. HPLC purity 98.1%. Yield 32.2%. <sup>1</sup>H NMR (400 MHz, DMSO-*d*<sub>6</sub>) $\delta$ : 12.95 (s, 1H), 10.18 (s, 1H), 9.01 (s, 1H), 8.61 (s, 1H), 7.93 (d,  $J = 6.5$  Hz, 2H), 7.85 (d,  $J = 7.9$  Hz, 1H), 7.61 (t,  $J = 8.0$  Hz, 1H), 7.11 (s, 1H), 5.90 (s, 1H), 5.60 (s, 1H), 1.99 (s, 3H). HRMS (ESI),  $m/z$ : 301.1014 [M + Na]<sup>+</sup>.

(*E*)-*N*-(3-(7*H*-Pyrrolo[2,3-*d*]pyrimidin-4-yl)phenyl)but-2-enamide (**T17**). White solid. HPLC purity 98.9%. Yield 31.4%. <sup>1</sup>H NMR (400 MHz, DMSO-*d*<sub>6</sub>) $\delta$ : 13.30 (s, 1H), 10.60 (s, 1H), 9.08 (s, 1H), 8.65 (s, 1H), 8.02 (d,  $J = 2.4$  Hz, 1H), 7.91 (d,  $J = 8.0$  Hz, 1H), 7.82 (d,  $J = 7.8$  Hz, 1H), 7.63 (t,  $J = 7.9$  Hz, 1H), 7.15 (d,  $J = 2.3$  Hz, 1H), 6.87 (dq,  $J = 13.8, 6.8$  Hz, 1H), 6.25 (dd,  $J = 15.2, 1.5$  Hz, 1H), 1.90 (dd,  $J = 6.8, 1.1$  Hz, 2H). HRMS (ESI),  $m/z$ : 279.0935 [M + H]<sup>+</sup>.

*N*-(3-(7*H*-Pyrrolo[2,3-*d*]pyrimidin-4-yl)phenyl)-3-methylbut-2-enamide (**T18**). White solid. HPLC purity 99.0%. Yield 35.0%. <sup>1</sup>H NMR (400 MHz, DMSO-*d*<sub>6</sub>) $\delta$ : 13.32 (s, 1H), 10.40 (s, 1H), 9.08 (s, 1H), 8.59 (d,  $J = 16.9$  Hz, 1H), 8.05–8.00 (m, 1H), 7.88 (d,  $J = 8.1$  Hz, 1H), 7.79 (d,  $J = 7.9$  Hz, 1H), 7.62 (t,  $J = 7.9$  Hz, 1H), 7.14 (d,  $J = 2.2$  Hz, 1H), 5.98 (s, 1H), 2.19 (s, 3H), 1.90 (s, 3H). HRMS (ESI),  $m/z$ : 293.1214 [M + H]<sup>+</sup>.

*N*-(3-(7*H*-Pyrrolo[2,3-*d*]pyrimidin-4-yl)phenyl)-2-chloroacetamide (**T19**). White solid. HPLC purity 97.1%. Yield 29.7%. <sup>1</sup>H NMR (400 MHz, DMSO-*d*<sub>6</sub>) $\delta$ : 12.30 (s, 1H), 10.56 (s, 1H), 8.84 (s, 1H), 8.54 (s, 1H), 7.94 (d,  $J = 7.6$  Hz, 1H), 7.75 (d,  $J = 8.4$  Hz, 1H), 7.70 (s, 1H), 7.55 (t,  $J = 7.9$  Hz, 1H), 6.94 (s, 1H), 4.32 (s, 2H). HRMS (ESI),  $m/z$ : 309.0512 [M + Na]<sup>+</sup>.

*N*-(3-(7*H*-Pyrrolo[2,3-*d*]pyrimidin-4-yl)phenyl)-2-bromoacetamide (**T20**). Light yellow solid. HPLC purity 95.4%. Yield 29.7%. <sup>1</sup>H NMR (400 MHz, DMSO-*d*<sub>6</sub>) $\delta$ : 12.31 (s, 1H), 10.57 (s, 1H), 8.84 (s, 1H), 8.78 (s, 1H), 8.55 (s, 1H), 7.95 (d,  $J = 7.7$  Hz, 1H), 7.75 (d,  $J = 7.8$  Hz, 1H), 7.71 (s, 1H), 7.55 (t,  $J = 7.9$  Hz, 1H), 6.95 (s, 1H), 4.32 (s, 2H). HRMS (ESI),  $m/z$ : 353.0007 [M + Na]<sup>+</sup>.

*N*-(3-(7*H*-Pyrrolo[2,3-*d*]pyrimidin-4-yl)phenyl)-2-chloropropanamide (**T21**). White solid. HPLC purity 97.2%. Yield 30.2%. <sup>1</sup>H NMR (400 MHz, DMSO-*d*<sub>6</sub>) $\delta$ : 12.35 (s, 1H), 10.63 (s, 1H), 8.90 (s, 1H), 8.64 (s, 1H), 8.01 (d,  $J = 7.9$  Hz, 1H), 7.87–7.80 (m, 1H), 7.76 (s, 1H), 7.61 (s, 1H), 7.01 (dd,  $J = 3.5, 1.6$  Hz, 1H), 4.78 (q,  $J = 6.6$  Hz, 1H), 1.72 (d,  $J = 6.7$  Hz, 3H). HRMS (ESI),  $m/z$ : 301.1402 [M + H]<sup>+</sup>.

*N*-(3-(6,7-Dihydro-5*H*-pyrrolo[2,3-*d*]pyrimidin-4-yl)phenyl)acrylamide (**T22**). White solid. HPLC purity 98.3%. Yield 33.4%. <sup>1</sup>H NMR (400 MHz, DMSO-*d*<sub>6</sub>) $\delta$ : 10.79 (s, 1H), 9.83 (s, 1H), 8.60 (s, 1H), 8.30 (s, 1H), 7.82 (d,  $J = 8.0$  Hz, 1H), 7.58 (t,  $J = 7.9$  Hz, 1H), 7.49 (d,  $J = 7.8$  Hz, 1H), 6.56 (dd,  $J = 17.0, 10.2$  Hz, 1H), 6.30 (dd,  $J = 17.0, 1.8$  Hz, 1H), 5.80 (dd,  $J = 10.2, 1.8$  Hz, 1H),

3.86 (t,  $J = 8.3$  Hz, 2H), 3.36 (t,  $J = 8.3$  Hz, 2H). HRMS (ESI),  $m/z$ : 267.0638 [M + H]<sup>+</sup>.

*N*-(3-(6,7-Dihydro-5*H*-pyrrolo[2,3-*d*]pyrimidin-4-yl)phenyl)methacrylamide (**T23**). White solid. HPLC purity 98.3%. Yield 33.7%. <sup>1</sup>H NMR (400 MHz, DMSO-*d*<sub>6</sub>) $\delta$ : 10.13 (s, 1H), 9.72 (s, 1H), 8.60 (s, 1H), 8.25 (s, 1H), 7.83 (d,  $J = 8.1$  Hz, 1H), 7.57 (t,  $J = 8.0$  Hz, 1H), 7.47 (d,  $J = 7.8$  Hz, 1H), 5.86 (s, 2H), 5.59 (s, 1H), 3.85 (t,  $J = 8.1$  Hz, 2H), 3.34 (t,  $J = 8.1$  Hz, 2H), 1.97 (s, 3H). HRMS (ESI),  $m/z$ : 319.1315 [M + K]<sup>+</sup>.

(*E*)-*N*-(3-(6,7-Dihydro-5*H*-pyrrolo[2,3-*d*]pyrimidin-4-yl)phenyl)but-2-enamide (**T24**). White solid. HPLC purity 98.5%. Yield 32.9%. <sup>1</sup>H NMR (400 MHz, DMSO)  $\delta$ : 10.63 (s, 1H), 9.88 (s, 1H), 8.60 (s, 1H), 8.29 (s, 1H), 7.82 (d,  $J = 7.8$  Hz, 1H), 7.55 (t,  $J = 7.9$  Hz, 1H), 7.47 (d,  $J = 7.8$  Hz, 1H), 6.84 (dd,  $J = 15.2, 6.9$  Hz, 1H), 6.25 (dd,  $J = 15.2, 1.5$  Hz, 1H), 3.86 (t,  $J = 8.1$  Hz, 2H), 3.35 (t,  $J = 8.2$  Hz, 2H), 1.90–1.84 (m, 3H). HRMS (ESI),  $m/z$ : 281.1402 [M + H]<sup>+</sup>.

*N*-(3-(6,7-Dihydro-5*H*-pyrrolo[2,3-*d*]pyrimidin-4-yl)phenyl)-3-methylbut-2-enamide (**T25**). White solid. HPLC purity 98.0%. Yield 31.5%. <sup>1</sup>H NMR (400 MHz, DMSO-*d*<sub>6</sub>)  $\delta$ : 10.27 (s, 1H), 9.82 (s, 1H), 8.62 (s, 1H), 8.24 (s, 1H), 7.71 (d,  $J = 8.1$  Hz, 1H), 7.54 (t,  $J = 7.9$  Hz, 1H), 7.41 (d,  $J = 8.0$  Hz, 1H), 5.92 (s, 1H), 3.86 (t,  $J = 8.4$  Hz, 2H), 3.33 (t,  $J = 8.3$  Hz, 2H), 2.17 (s, 3H), 1.89 (s, 3H). HRMS (ESI),  $m/z$ : 295.0978 [M + H]<sup>+</sup>.

2-Chloro-*N*-(3-(6,7-dihydro-5*H*-pyrrolo[2,3-*d*]pyrimidin-4-yl)phenyl)acetamide (**T26**). White solid. HPLC purity 96.1%. Yield 31.5%. <sup>1</sup>H NMR (400 MHz, DMSO-*d*<sub>6</sub>)  $\delta$ : 10.55 (s, 1H), 8.23 (s, 1H), 7.41 (s, 1H), 7.19 (s, 1H), 7.11 (t,  $J = 7.5$  Hz, 1H), 7.00 (d,  $J = 7.1$  Hz, 1H), 6.63 (d,  $J = 7.0$  Hz, 1H), 5.20 (s, 2H), 3.56 (t,  $J = 8.3$  Hz, 2H), 3.25 (t,  $J = 8.3$  Hz, 2H). HRMS (ESI),  $m/z$ : 311.1133 [M + Na]<sup>+</sup>.

2-Bromo-*N*-(3-(6,7-dihydro-5*H*-pyrrolo[2,3-*d*]pyrimidin-4-yl)phenyl)acetamide (**T27**). White solid. HPLC purity 95.4%. Yield 28.5%. <sup>1</sup>H NMR (400 MHz, DMSO-*d*<sub>6</sub>)  $\delta$ : 10.55 (s, 1H), 8.23 (s, 1H), 7.39 (s, 1H), 7.18 (s, 1H), 7.10 (t,  $J = 7.8$  Hz, 1H), 7.00 (d,  $J = 7.8$  Hz, 1H), 6.62 (d,  $J = 9.5$  Hz, 1H), 5.18 (s, 2H), 3.55 (t,  $J = 8.3$  Hz, 2H), 3.25 (t,  $J = 8.3$  Hz, 2H). HRMS (ESI),  $m/z$ : 333.0384 [M + H]<sup>+</sup>.

2-Chloro-*N*-(3-(6,7-dihydro-5*H*-pyrrolo[2,3-*d*]pyrimidin-4-yl)phenyl)propanamide (**T28**). White solid. HPLC purity 96.7%. Yield 24.9%. <sup>1</sup>H NMR (400 MHz, DMSO-*d*<sub>6</sub>)  $\delta$ : 10.53 (s, 1H), 8.27 (d,  $J = 4.2$  Hz, 2H), 7.71 (d,  $J = 8.0$  Hz, 1H), 7.65 (d,  $J = 7.9$  Hz, 1H), 7.54 (s, 1H), 7.45 (t,  $J = 7.9$  Hz, 1H), 4.71 (q,  $J = 6.6$  Hz, 1H), 3.60 (t,  $J = 8.4$  Hz, 2H), 3.31 (d,  $J = 8.5$  Hz, 2H), 1.63 (d,  $J = 6.6$  Hz, 3H). HRMS (ESI),  $m/z$ : 325.0836 [M + Na]<sup>+</sup>.

*N*-(3-(1*H*-Pyrrolo[2,3-*b*]pyridin-4-yl)phenyl)acrylamide (**T29**). White solid. HPLC purity 99.3%. Yield 33.9%. <sup>1</sup>H NMR (400 MHz, DMSO-*d*<sub>6</sub>) $\delta$ : 11.87 (s, 1H), 10.40 (s, 1H),

8.35 (d,  $J = 4.9$  Hz, 1H), 8.29 (s, 1H), 7.81–7.76 (m, 1H), 7.66–7.61 (m, 1H), 7.59–7.51 (m, 2H), 7.25 (d,  $J = 4.9$  Hz, 1H), 6.76 (dd,  $J = 3.4, 1.8$  Hz, 1H), 6.53 (dd,  $J = 17.0, 10.1$  Hz, 1H), 6.36 (dd,  $J = 17.0, 2.0$  Hz, 1H), 5.85 (dd,  $J = 10.1, 2.0$  Hz, 1H). <sup>13</sup>C NMR (101 MHz, DMSO-*d*<sub>6</sub>)  $\delta$ : 168.68, 163.83, 149.67, 143.38, 140.43, 139.9, 139.34 (s, 1H), 129.94, 127.14, 123.50, 119.47, 117.64, 114.41, 99.55. HRMS (ESI),  $m/z$ : 264.1132 [M + H]<sup>+</sup>.

*N*-(3-(1*H*-Pyrrolo[2,3-*b*]pyridin-4-yl)phenyl)methacrylamide (**T30**). White solid. HPLC purity 98.7%. Yield 34.8%. <sup>1</sup>H NMR (400 MHz, DMSO-*d*<sub>6</sub>) $\delta$ : 11.86 (s, 1H), 10.03 (s, 1H), 8.34 (d,  $J = 4.8$  Hz, 1H), 8.28 (s, 1H), 7.83 (d,  $J = 7.1$  Hz, 1H), 7.63 (s, 1H), 7.59–7.49 (m, 2H), 7.25 (d,  $J = 4.8$  Hz, 1H), 6.78 (s, 1H), 5.91 (s, 1H), 5.61 (s, 1H), 2.04 (s, 3H). HRMS (ESI),  $m/z$ : 278.1296 [M + H]<sup>+</sup>.

*N*-(3-(1*H*-Pyrrolo[2,3-*b*]pyridin-4-yl)phenyl)-2-chloroacetamide (**T31**). White solid. HPLC purity 97.0%. Yield 35.0%. <sup>1</sup>H NMR (400 MHz, DMSO-*d*<sub>6</sub>)  $\delta$ : 11.83 (s, 1H), 10.51 (s, 1H), 8.30 (d,  $J = 4.9$  Hz, 1H), 8.14 (s, 1H), 7.66 (d,  $J = 7.1$  Hz, 1H), 7.59–7.56 (m, 1H), 7.53–7.50 (m, 2H), 7.20 (d,  $J = 4.9$  Hz, 1H), 6.71–6.66 (m, 1H), 4.31 (s, 2H). HRMS (ESI),  $m/z$ : 286.0750 [M + H]<sup>+</sup>.

*N*-(3-(1*H*-Pyrrolo[2,3-*b*]pyridin-4-yl)phenyl)-2-bromoacetamide (**T32**). White solid. HPLC purity 96.3%. Yield 30.9%. <sup>1</sup>H NMR (400 MHz, DMSO-*d*<sub>6</sub>)  $\delta$ : 11.79 (s, 1H), 10.51 (s, 1H), 8.29 (d,  $J = 4.9$  Hz, 1H), 8.19 (s, 1H), 7.74 (d,  $J = 6.6$  Hz, 1H), 7.59–7.53 (m, 1H), 7.48 (d,  $J = 6.3$  Hz, 2H), 7.18 (d,  $J = 4.9$  Hz, 1H), 6.71 (s, 1H), 4.31 (s, 2H). HRMS (ESI),  $m/z$ : 330.0240 [M + H]<sup>+</sup>.

*N*-(3-(1*H*-Pyrrolo[2,3-*b*]pyridin-4-yl)phenyl)-2-chloropropanamide (**T33**). White solid. HPLC purity 96.9%. Yield 29.1%. <sup>1</sup>H NMR (400 MHz, DMSO-*d*<sub>6</sub>)  $\delta$ : 11.82 (s, 1H), 10.58 (s, 1H), 8.30 (s, 0H), 8.16 (s, 0H), 7.68 (s, 1H), 7.58 (s, 1H), 7.51 (d,  $J = 5.5$  Hz, 1H), 7.20 (s, 0H), 6.69 (s, 0H), 4.73 (s, 1H), 1.64 (d,  $J = 6.2$  Hz, 1H). HRMS (ESI),  $m/z$ : 322.0721 [M + Na]<sup>+</sup>.

**Enzymatic assays** The enzymatic activities against JAK1, JAK2, JAK3, and TYK2 were assessed using the Caliper Mobility Shift Assay in the presence of *K<sub>m</sub>* ATP (ChemPartner, Shanghai, China). The assay protocol guide is commercially available from ChemPartner. The inhibitory activities against cysteine kinome were tested by Eurofins Cerep (CEREP, Celle l'Evescault, France). The protocols are available from <http://www.cerep.fr/Cerep/Users/index.asp>. The assay protocol guide can be accessed at [www.eurofins.com/discovery](http://www.eurofins.com/discovery).

**Evaluation of anti-inflammatory activity in ICR mice** ICR mice were randomized into five groups ( $n = 6$ ) and labeled with picric acid. Mice in treatment groups were orally administered with corresponding inhibitors at a single dose of 30 mg/kg. After 30 min, all mice were injected carrageenan and this time point was recorded as 0 h. The data of paw size

were measured and collected at 0, 1, 2, 3, 4, and 5 h, and then the data were described as a figure.

**JAK3 reversibility experiments** Jump dilution [13,26] was used to assess the reversibility of **T29** binding to JAK3. Prepare enzyme mixes in 1× kinase buffer (50 mM HEPES, pH 7.5, 0.0015% Brij-35, 10 mM MgCl<sub>2</sub>, 2 mM DTT) and incubate enzyme mix at r.t. for 30 min: Enzyme mix 1 contains 75X JAK3 (300 nM) of final concentration in reaction; enzyme mix 2 contains 75X JAK3 (300 nM) and compound **T29** at high concentration 20X IC<sub>50</sub> (2.8 nM). Prepare substrate mix in 1× kinase buffer: Substrate mix 1 contains peptide substrate, ATP, and cofactors at the final concentration for reaction; substrate mix 2 contains peptide substrate, ATP, and cofactors at the concentration for reaction with extremely low concentration 20/74X IC<sub>50</sub> of compound **T29** (0.037 nM). Transfer 1 μL enzyme mix and 74 μL substrate mix to the 384-well assay plate: no compound (enzyme mix 1 + substrate mix 1); **T29** with pre-incubation (enzyme mix 2 + substrate mix 1); **T29** without pre-incubation (enzyme mix 1 + substrate mix 2); no enzyme (buffer + substrate mix 1). Then, continually read each well for 20 times for 1 h on caliper, collect JAK3 conversion data, and describe as a figure.

**Covalent in silico docking** The crystal structure of the JAK3 kinase domain was obtained from the Protein Data Bank (PDB code 1YVJ) [27]. Water molecules were removed, and hydrogen atoms were added to the structure. Three-dimensional structure of the compounds were generated and optimized by the Discovery Studio 3.1 package (Accelrys, San Diego, CA, USA). The small molecule was docked into the JAK3 kinase domain using the Covalent Dock Cloud server (<http://docking.sce.ntu.edu.sg>) [28]. Figure 4 was generated using Pymol 1.7.

**Acknowledgements** The authors greatly appreciate the financial support from the National Natural Science Foundation of China (81373260).

## Compliance with ethical standards

**Conflict of interest** The authors have declared no conflict of interest.

## References

- Hanan EJ, Abbema A, Barrett K, Blair WS, Blaney J, Chang C, Eigenbrot C, Flynn S, Gibbons P, Hurley CA, Kenny JR, Kulagowski J, Lee L, Magnuson SR, Morris C, Murray J, Pastor RM, Rawson T, Siu M, Ultsch M, Zhou A, Sampath D, Lyssikatos JP (2012) Discovery of potent and selective pyrazolopyrimidine Janus kinase 2 inhibitors. *J Med Chem* 55:10090–10107. <https://doi.org/10.1021/jm3012239>
- Thoma G, Druckes P, Zerwes H (2014) Selective inhibitors of the Janus kinase Jak3—are they effective? *Bioorg Med Chem Lett* 24:4617–4621. <https://doi.org/10.1016/j.bmcl.2014.08.046>
- Jasuja H, Chadha N, Kaur M, Silakari O (2014) Dual inhibitors of Janus kinase 2 and 3 (JAK2/3): designing by pharmacophore- and docking-based virtual screening approach. *Mol Divers* 18:253–267. <https://doi.org/10.1007/s11030-013-9497-z>
- Farmer LJ, Ledebroer MW, Hoock T, Arnost MJ, Bethiel RS, Ben-nani YL, Black JJ, Brummel CL, Chakilam A, Dorsch WA, Fan B, Cochran JE, Halas S, Harrington EM, Hogan JK, Howe D, Huang H, Jacobs DH, Laitinen LM, Liao S, Mahajan S, Marone V, Martinez-Botella G, McCarthy P, Messersmith D, Namchuk M, Oh L, Penney MS, Pierce AC, Raybuck SA, Rugg A, Salituro FG, Saxena K, Shannon D, Shlyakter D, Swenson L, Tian SK, Town C, Wang J, Wang T, Wannamaker MW, Winquist RJ, Zuccola HJ (2015) Discovery of VX-509 (decernotinib): a potent and selective Janus kinase 3 inhibitor for the treatment of autoimmune diseases. *J Med Chem* 58:7195–7216. <https://doi.org/10.1021/acs.jmedchem.5b00301>
- Villarino AV, Kanno Y, Ferdinand JR, O'Shea JJ (2015) Mechanisms of Jak/STAT signaling in immunity and disease. *J Immunol* 194:21–27. <https://doi.org/10.4049/jimmunol.1401867>
- Clark JD, Flanagan ME, Telliez J (2014) Discovery and development of Janus kinase (JAK) inhibitors for inflammatory diseases. *J Med Chem* 57:5023–5038. <https://doi.org/10.1021/jm401490p>
- Madan B, Goh KC, Hart S, William AD, Jayaraman R, Ethirajulu K, Dymock BW, Wood JM (2012) SB1578, a novel inhibitor of JAK2, FLT3, and c-Fms for the treatment of rheumatoid arthritis. *J Immunol* 189:4123–4134. <https://doi.org/10.4049/jimmunol.1200675>
- Hill RJ, Bisconte A, Bradshaw JM, Brameld K, Kim EO, Li X, Owens T, Verner E, Goldstein DM (2012) Discovery of a highly potent, selective, reversible covalent inhibitor of JAK3. Principia Biopharma. [www.principiabiobio.com](http://www.principiabiobio.com), <http://www.principiabiobio.com/file.cfm/8/docs/JAK3%20poster%20ACR%202012%20Final.pdf>
- O'Shea JJ, Schwartz DM, Villarino AV, Gadina M, McInnes IB, Laurence A (2015) The JAK–STAT pathway: impact on human disease and therapeutic intervention. *Annu Rev Med* 66:311–328. <https://doi.org/10.1146/annurev-med-051113-024537>
- Tan L, Akahane K, McNally R, Reyskens KM, Ficarro SB, Liu S, Herter-Sprie GS, Koyama S, Pattison MJ, Labella K, Johannessen L, Akbay EA, Wong KK, Frank DA, Marto JA, Look TA, Arthur JS, Eck MJ, Gray NS (2015) Development of selective covalent Janus kinase 3 inhibitors. *J Med Chem* 58:6589–6606. <https://doi.org/10.1021/acs.jmedchem.5b00710>
- Flanagan ME, Blumenkopf TA, Brissette WH, Brown MF, Casavant JM, Shang-Poa C, Doty JL, Elliott EA, Fisher MB, Hines M, Kent C, Kudlacz EM, Lillie BM, Magnuson KS, McCurdy SP, Munchhof MJ, Perry BD, Sawyer PS, Strelevitz TJ, Subramanyam C, Sun J, Whipple DA, Changelian PS (2010) Discovery of CP-690,550: a potent and selective Janus kinase (JAK) inhibitor for the treatment of autoimmune diseases and organ transplant rejection. *J Med Chem* 53:8468–8484. <https://doi.org/10.1021/jm1004286>
- Van Rompaey L, Galien R, van der Aar EM, Clement-Lacroix P, Nelles L, Smets B, Lepescheux L, Christophe T, Conrath K, Vandeghinste N, Vayssiere B, De Vos S, Fletcher S, Brys R, van 't Klooster G, Feyen JH, Menet C (2013) Preclinical characterization of GLPG0634, a selective inhibitor of JAK1, for the treatment of inflammatory diseases. *J Immunol* 191:3568–3577. <https://doi.org/10.4049/jimmunol.1201348>
- Kulagowski JJ, Blair W, Bull RJ, Chang C, Deshmukh G, Dyke HJ, Eigenbrot C, Ghilardi N, Gibbons P, Harrison TK, Hewitt PR, Liimatta M, Hurley CA, Johnson A, Johnson T, Kenny JR, Bir Kohli P, Maxey RJ, Mendonca R, Mortara K, Murray J, Narukulla R, Shia S, Steffek M, Ubhayakar S, Ultsch M, van Abbema A, Ward SI, Waszkowycz B, Zak M (2012) Identification of imidazopyrrolopyridines as novel and potent JAK1 inhibitors. *J Med Chem* 55:5901–5921. <https://doi.org/10.1021/jm300438j>

14. Goedken ER, Argiriadi MA, Banach DL, Fiamengo BA, Foley SE, Frank KE, George JS, Harris CM, Hobson AD, Ihle DC, Marcotte D, Merta PJ, Michalak ME, Murdock SE, Tomlinson MJ, Voss JW (2014) Tricyclic covalent inhibitors selectively target Jak3 through an active-site thiol. *J Biol Chem* 290:4573–4589. <https://doi.org/10.1074/jbc.M114.595181>
15. Meyer DM, Jesson MI, Li X, Elrick MM, Funckes-Shippy CL, Warner JD, Gross CJ, Dowty ME, Ramaiah SK, Hirsch JL, Saabye MJ, Barks JL, Kishore N, Morris DL (2010) Anti-inflammatory activity and neutrophil reductions mediated by the JAK1/JAK3 inhibitor, CP-690,550, in rat adjuvant-induced arthritis. *J Inflamm* 7:41. <https://doi.org/10.1186/1476-9255-7-41>
16. Changelian PS, Flanagan ME, Ball DJ, Kent CR, Magnuson KS, Martin WH, Rizzuti BJ, Sawyer PS, Perry BD, Brissette WH, McCurdy SP, Kudlacz EM, Conklyn MJ, Elliott EA, Koslov ER, Fisher MB, Strelevitz TJ, Yoon K, Whipple DA, Sun J, Munchhof MJ, Doty JL, Casavant JM, Blumenkopf TA, Hines M, Brown MF, Lillie BM, Subramanyam C, Shang-Poa C, Milici AJ, Beckius GE, Moyer JD, Su C, Woodworth TG, Gaweco AS, Beals CR, Littman BH, Fisher DA, Smith JF, Zagouras P, Magna HA, Saltarelli MJ, Johnson KS, Nelms LF, Des Etages SG, Hayes LS, Kawabata TT, Finco-Kent D, Baker DL, Larson M, Si MS, Paniagua R, Higgins J, Holm B, Reitz B, Zhou YJ, Morris RE, O'Shea JJ, Borie DC (2003) Prevention of organ allograft rejection by a specific Janus kinase 3 inhibitor. *Science* 302:875–878. <https://doi.org/10.1126/science.1087061>
17. Scott LJ (2013) Tofacitinib: a review of its use in adult patients with rheumatoid arthritis. *Drugs* 73:857–874. <https://doi.org/10.1007/s40265-013-0065-8>
18. Simmons DL (2013) Targeting kinases: a new approach to treating inflammatory rheumatic diseases. *Curr Opin Pharmacol* 13:426–434. <https://doi.org/10.1016/j.coph.2013.02.008>
19. Williams NK, Bamert RS, Patel O, Wang C, Walden PM, Wilks AF, Fantino E, Rossjohn J, Lucet IS (2009) Dissecting specificity in the Janus kinases: the structures of JAK-specific inhibitors complexed to the JAK1 and JAK2 protein tyrosine kinase domains. *J Mol Biol* 387:219–232. <https://doi.org/10.1016/j.jmb.2009.01.041>
20. Gehringer M, Forster M, Pfaffenrot E, Bauer SM, Laufer SA (2014) Novel hinge-binding motifs for Janus kinase 3 inhibitors: a comprehensive structure–activity relationship study on tofacitinib bioisosteres. *Chem Med Chem* 9:2516–2527. <https://doi.org/10.1002/cmdc.201402252>
21. Thorarensen A, Dowty ME, Banker ME, Juba B, Jussif J, Lin T, Vincent F, Czerwinski RM, Casimiro-Garcia A, Unwalla R, Trujillo JI, Liang S, Balbo P, Che Y, Gilbert AM, Brown MF, Hayward M, Montgomery J, Leung L, Yang X, Soucy S, Hegen M, Coe J, Langille J, Vajdos F, Chrencik J, Telliez JB (2017) Design of a Janus kinase 3 (JAK3) specific inhibitor 1((2*S*,5*R*)-5-((7*H*-pyrrolo[2,3*d*]pyrimidin-4-yl)amino)-2-methylpiperidin-1-yl)prop-2-en-1-one(PF-06651600) allowing for the interrogation of JAK3 signaling in humans. *J Med Chem* 60:1971–1993. <https://doi.org/10.1021/acs.jmedchem.6b01694>
22. Smith GA, Uchida K, Weiss A, Taunton J (2016) essential biphasic role for Jak3 catalytic activity in IL-2 receptor signaling. *J Nat Chem Biol* 12:373–379. <https://doi.org/10.1038/nChEMBio.2056>
23. Telliez J, Dowty ME, Wang L, Jussif J, Lin T, Moy E, Balbo P, Li W, Zhao Y, Crouse K, Dickinson C, Symanowicz P, Hegen M, Banker ME, Vincent F, Unwalla R, Liang S, Gilbert AM, Brown MF, Hayward M, Montgomery J, Yang X, Bauman J, Trujillo JI, Casimiro-Garcia A, Vajdos FF, Leung L, Geoghegan KF, Quazi A, Xuan D, Jones L, Hett E, Wright K, Clark JD, Thorarensen A (2016) Discovery of a JAK3-selective inhibitor: functional differentiation of JAK3-selective inhibition over pan-JAK or JAK1-selective inhibition. *ACS Chem Biol* 11:3442–3451. <https://doi.org/10.1021/acschembio.6b00677>
24. Lima LM, Barreiro EJ (2005) Bioisosterism: a useful strategy for molecular modification and drug design. *Curr Med Chem* 12:23–49. <https://doi.org/10.2174/0929867053363540>
25. Barf T, Kaptein A (2012) Irreversible protein kinase inhibitors: balancing the benefits and risks. *J Med Chem* 55:6243–6262. <https://doi.org/10.1021/jm3003203>
26. Copeland RA, Basavapathruni A, Moyer M, Scott MP (2011) Impact of enzyme concentration and residence time on apparent activity recovery in jump dilution analysis. *Anal Biochem* 416:206–210
27. Boggon TJ, Li Y, Manley PW, Eck MJ (2005) Crystal structure of the Jak3 kinase domain in complex with a staurosporine analog. *Blood* 106:996–1002. [10.1182/blood-2005-02-0707](https://doi.org/10.1182/blood-2005-02-0707)
28. Ouyang X, Zhou S, Su CTT, Ge Z, Li R, Kwok CK (2013) Covalent dock: automated covalent docking with parameterized covalent linkage energy estimation and molecular geometry constraints. *J Comput Chem* 34:326–336. <https://doi.org/10.1002/jcc.23136>